

**A Study of the Potential Use of an Energy Based  
Motion Parameter for Probabilistic Determination  
of Scenario Earthquakes**

**Grant Award No. 1434-HQ-97-GR-03067**

**Martin C. Chapman and J. Arthur Snoke**

**Virginia Polytechnic Institute and State University**

**Department of Geological Sciences**

**Blacksburg, VA 24061**

**NEHRP Element I: Evaluating National and Regional Hazard and Risk**

**Research supported by the U. S. Geological Survey (USGS), Department of the Interior, under USGS award number 1434-HQ-97-GR-03067. The views and conclusions contained in this document are those of the authors and should not be interpreted as necessarily representing the official policies, either expressed or implied, of the U. S. Government.**

Grant Award Number: 1434-HQ-97-GR-03067

A STUDY OF THE POTENTIAL USE OF AN ENERGY BASED MOTION  
PARAMETER FOR DETERMINATION OF SCENARIO EARTHQUAKES

M. C. Chapman and J. Arthur Snoke

Department of Geological Sciences, Virginia Polytechnic Institute and State University,  
Blacksburg, VA 24061.

Phone: (540) 231-5036, fax: (540) 231-3386, E-mail: chapman@vtso.geol.vt.edu

Phone: (540) 231-6028, fax (540) 231-3386, E-mail: snoke@vt.edu

**TECHNICAL ABSTRACT**

Amplitude and duration of strong motion are important considerations for engineering analysis. However, duration is not modeled routinely in seismic hazard assessments. Probabilistic assessment based on elastic input-energy may prove useful in the identification of scenario events, because input-energy depends on duration and amplitude. To investigate this application, regression models are derived for the elastic input-energy spectrum using data from western U.S. earthquakes. Those results are compared with *PSV* response spectra derived from the same data set, in terms of effect on disaggregated seismic hazard for generalized cases.

Similar regression models were used for *PSV* spectra and equivalent velocity spectra derived from the absolute and relative input-energy spectra. Variances of the regressions systematically decrease with increasing oscillator frequency in the range 0.5 to 5 Hz. In that frequency range, variance associated with the energy parameter is slightly smaller than for *PSV*. Response differences due to NEHRP site class are largest at the lowest frequencies, for both energy and *PSV* models. The energy models are almost independent of site class for frequencies greater than approximately 4 Hz. The energy models show stronger dependence upon earthquake magnitude, compared to *PSV*: the ratio of the equivalent velocity spectral amplitudes to the *PSV* amplitudes increases with magnitude. Also, that ratio increases with distance for frequencies in the range 0.5 to 7 Hz. These results are attributable to duration of shaking. The effect upon hazard is such that larger, more distant earthquakes typically contribute significantly more to the total hazard, for any given return period, when the hazard model is based upon the energy parameter, rather than *PSV*. This effect is most pronounced at the higher oscillator frequencies, in the range 3 to 10 Hz.

#### **NON-TECHNICAL ABSTRACT**

The disaggregation of probabilistic seismic hazard calculations based on elastic input energy may prove useful for the identification of scenario events because input energy is a convenient single-parameter descriptor of motion duration and amplitude. To investigate this application, regression models are derived for the absolute input energy equivalent velocity,  $V_{ea}$ , and the elastic pseudo-relative velocity response,  $PSV$ , in the frequency range 0.5 to 10 Hz. Disaggregation of a general seismic hazard model using  $V_{ea}$  indicates that the modal magnitudes for the higher frequency oscillators tend to be larger, and vary less with oscillator frequency, than those derived using  $PSV$ . The dependence of  $V_{ea}$  and  $PSV$  upon site classification is virtually identical, and  $V_{ea}$  can be predicted with slightly less uncertainty as a function of magnitude, distance and site classification.

## INTRODUCTION

It is often desirable to base the selection of scenario earthquakes for engineering design upon a probabilistic estimate of the seismic hazard. A scenario event, defined by magnitude and distance from a site, can provide a starting point for selection or synthesis of ground motion time series to be used for a variety of dynamic analyses. Information for this choice can be extracted from a probabilistic model of the seismic hazard by an analysis known as "disaggregation". Recently, approaches to disaggregation have received considerable attention and application (e.g., Stepp et al. 1993; Chapman 1995; McGuire 1995; Cramer and Petersen 1996; Bazzurro and Cornell 1998a, 1998b; Harmsen et al. 1998). The results of the disaggregation provide much insight into the nature of hazard at a given site, and the choice of scenario earthquakes may be guided by those combinations of earthquake magnitude and source-site distance that have the most significant contributions to seismic hazard for a selected probability of exceedance.

The probabilistic seismic hazard analysis (PSHA) requires a model from which median estimates of a strong motion parameter can be derived as a function of magnitude, distance and perhaps other variables such as site condition and type of faulting. The model must provide an estimate of the statistical variability of the parameter. Most suitable motion prediction models currently available yield estimates of peak ground motion values or peak response of elastic, single-degree-of-freedom (SDOF) oscillators. Such measures of motion are essentially independent of the duration of the ground motion. Recent work (Shome et al. 1998; Shome and Cornell 1998), using scaled strong motion recordings from earthquakes over a large range of magnitudes, indicates that maximum post-elastic displacement (ductility) response is largely independent of duration. On the other hand, some less commonly used structural response measures, such as cumulative hysteretic energy, are dependent upon duration. Some geotechnical problems involve consideration of cumulative deformation and the effects of repeated loading cycles, in which case duration of motion may be important.

This study does not address the issue of appropriate damage measures for earthquake resistant design of different types of construction. It explores some aspects of using a parameter derived from the elastic input energy spectrum in probabilistic seismic hazard analysis. The motivation for this study is the fact that the input energy is a convenient single parameter descriptor of both the amplitude and duration of the motion, in terms of the work done on an elastic SDOF oscillator. For that reason it could potentially provide a useful basis for defining scenario events, particularly in the context of a disaggregated PSHA.

A comprehensive study by Lawson (1996) developed regression models for both elastic and inelastic input energy spectra, as well as elastic response spectra. The present study uses a similar, but somewhat larger, data set, comprised of western North American strong motion recordings. The focus of this study is on a comparison of the magnitude and distance dependence of the elastic input energy spectrum with the elastic *PSV* response which is often used in probabilistic hazard analysis. The objective is to assess the degree to which use of a duration dependent motion parameter changes the hazard results in regard to the "source" of seismic hazard at a given probability level. This is done by first developing representative motion prediction models for the two parameters, using identical data processing procedures, and then comparing the disaggregated results of a general seismic hazard model.

## STRONG MOTION DATA

The data set consists of horizontal component recordings from 23 earthquakes in western North America. Table A1 in the appendix lists the earthquakes, along with station names and site numbers, component azimuth, source to site distance, station coordinates and site classification. The source to station distance adopted for this study is that used by Boore et al. (1993, 1994 and 1997), and is the nearest horizontal distance from the station to the surface projection of the fault rupture. The site classification is that adopted by the NEHRP, (BSSC 1994; see also Boore et al. 1997) which is defined on the basis of average shear wave velocity in the upper 30 meters (Table 1).

Data selection and regression modeling used in this study follows closely the approach developed and used in previous work by Boore et al. (1993, 1994 and 1997) and Joyner and Boore (1993, 1994). The data were recorded at ground level or in basements of structures of two stories or less, and do not include records from dam or bridge abutments. For 17 of the 23 earthquakes, the data assembled here for analysis is a subset of that used and documented thoroughly by Boore et al. (1993, 1994 and 1997). The remaining data are recordings from the 1994 Northridge shock and from some recent shocks with magnitudes in the range 5.0 to 6.2 (Westmoreland, Morgan Hill, Whittier Narrows, Sierra Madre, and Big Bear).

The sources of strong motion data were the collection of recordings assembled and distributed by NOAA (Earthquake Strong Motion CD-ROM); and the internet websites maintained by the California Division of Mines and Geology strong motion instrumentation program, the U. S. Geological Survey national strong motion program and the Civil Engineering Department, University of Southern California. Table A1 identifies the source of the data, along with that organization's site identification number, as appearing in the data file header, if available.

Table 1. NEHRP\* site class

Site Class	Range of Shear Velocities
A	>1500 m/s
B	760 m/s to 1500 m/s
C	360 m/s to 760 m/s
D	180 m/s to 360 m/s
E	< 180 m/s

\* BSSC (1994)

The recordings were selected so as to include the major motion portion of the strong motion episode, represented by the S wavetrain. Recordings that triggered late on the S wave, or those of short duration terminating early in the coda, were not used. The iterative approach described by Campbell (1997) was used to reduce bias due to the effects of non-triggered instruments, in the data sets from some of the more recent shocks. Using predicted values of peak horizontal acceleration, a maximum acceptable distance is established as a function of data variance, earthquake magnitude and site classification. This will be discussed further below.

Corrected accelerogram data provided by the contributing sources comprise a large portion

of the assembled data set. However, a sizable fraction of the data was processed for this study. Evenly sampled, uncorrected data were available from the U. S. Geological Survey National Strong Motion Program (NSMP) for the Petrolia, Landers, Big Bear and Northridge earthquakes. Those data were instrument corrected and bandpassed using a 4-pole causal Butterworth filter with corner frequencies 0.1 and 25 Hz. Unevenly sampled, uncorrected data were available from the University of Southern California (USC) sites for the Whittier Narrows, Sierra Madre, Landers, Big Bear and Northridge earthquakes. Those data were interpolated and sampled evenly using a 0.005 s interval, and instrument corrected. A causal Butterworth bandpass filter with corner frequencies at 0.2 and 25 Hz was then applied. A 6-pole filter was used for the Landers and Big Bear data, whereas a 4-pole filter was used for the Whittier Narrows and Sierra Madre recordings.

In all cases, using corrected data from the contributing sources or data corrected as described above, the recordings were passed through a final filter stage consisting of a 6-pole, causal high-pass Butterworth filter, with corner frequency 0.2 Hz. The filter parameter selections were chosen to insure that low-frequency noise was suppressed. This was verified for all the data by visual inspection of integrated velocity and displacement recordings. The response and energy spectra derived from these data are considered reliable for oscillator frequencies greater than 0.5 Hz.

Site classification according to BSSC (1994) for the recording sites was obtained from compilations of Boore et al. (1993), Harmsen (1997) and Boore et al. (1997). Source to recording site distances for all earthquakes occurring prior to 1981, as well as for the Loma Prieta and Petrolia earthquakes, are taken from Boore et al. (1993, 1997). Site distances for the Westmoreland earthquake were calculated using the aftershock distribution as given by Sharp et al. (1986). Distances for the Morgan Hill earthquake were calculated from the aftershock distribution summarized by Cockerham and Eaton (1987). The aftershock distributions given by Hauksson (1994) were used to calculate the site distances for the Whittier Narrows and Sierra Madre earthquakes. Distances for the Landers and Big Bear earthquakes were derived from the aftershock distributions and the fault model of Wald and Heaton (1994). Distances for the Northridge earthquake were derived using the rupture model of Wald et al. (1996).

Figure 1 shows the distribution of data in terms of magnitude, distance and site classification. Site classes A and B are combined for analysis, because so few data are available.

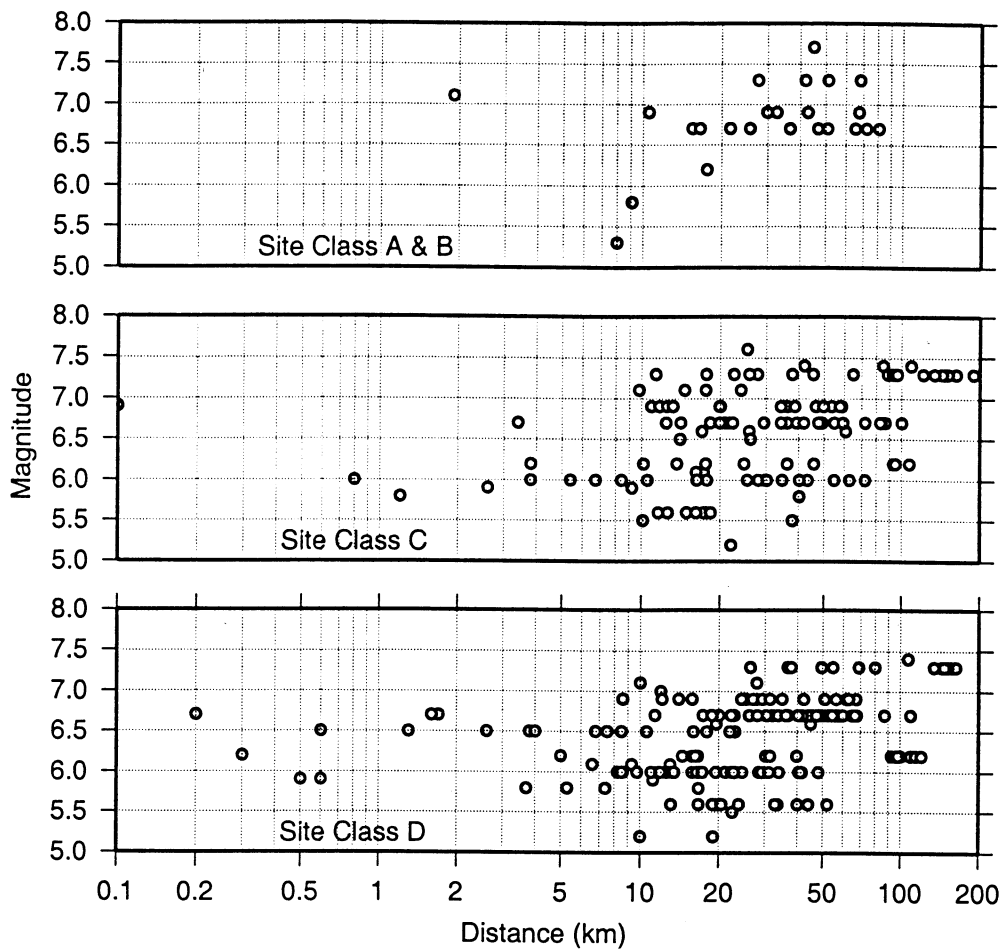


Figure 1. Distribution of data in terms of magnitude, distance and site classification. Top: site classes A and B, combined, n=24. Middle: site class C, n=116. Bottom: site class D, n=164.

## RESPONSE PARAMETERS

The emphasis of this study is on comparing the distance and magnitude dependence of maximum elastic oscillator response and input energy. Regression analysis is performed on peak horizontal ground acceleration  $PGA$ , peak horizontal ground velocity  $PGV$ , elastic oscillator  $PSV$  response and a parameter derived from the absolute input energy for elastic oscillators. The regression models are derived for a randomly oriented horizontal component, using the geometric mean of the two horizontal components.

The values of  $PGA$  and  $PGV$  used in this study are those values obtained from the corrected acceleration and integrated corrected acceleration recordings, following filtering as described above. Note that a small difference exists in the values of those parameters used in regression and the values of the original recordings.

The algorithm of Nigam and Jennings (1969) was used to calculate the elastic oscillator response time series necessary for construction of  $PSV$  and energy spectra.

### Input energy

Following Uang and Bertero (1990), the equation of motion of a damped SDOF system is

$$m(\ddot{x}_g + \ddot{x}) + c\dot{x} + f = 0. \quad (1)$$

Here,  $x_g$  is the displacement of the ground, and  $x$  is the relative displacement of the mass with respect to the ground,  $c$  is the damping coefficient and  $f$  is the restoring force. The equation of motion of an equivalent system with fixed base, acted upon by a force  $-m\ddot{x}_g$  is given by

$$m\ddot{x} + c\dot{x} + f = -m\ddot{x}_g. \quad (2)$$

Uang and Bertero (1990) show that the equivalent representations of the dynamic system lead to two definitions of input energy. Integrating (1) with respect to  $x$  leads to

$$m\dot{x}_t^2/2 + \int c\dot{x} dx + \int f dx = \int m\ddot{x}_t dx_g, \quad (3)$$

where  $x_t = x_g + x$ , is the total or absolute displacement. Integration of (2) with respect to  $x$  leads to

$$m\dot{x}^2/2 + \int c\dot{x} dx + \int f dx = -\int m\ddot{x}_g dx. \quad (4)$$

The RHS of (3) is known as the absolute input energy  $E_a$ , and can also be expressed as

$$E_a = \int m\ddot{x}_t dx_g = \int m\ddot{x}_t \dot{x}_g dt = \int m(\ddot{x} + \ddot{x}_g)\dot{x}_g dt. \quad (5)$$

The RHS of equation 4 is the relative input energy  $E_r$ , which can be written as

$$E_r = -\int m\ddot{x}_g dx = -\int m\ddot{x}_g \dot{x} dt. \quad (6)$$

Note that the damping and strain energy terms are the same in equations 3 and 4, and that the distinction between "absolute" and "relative" applies to the input and kinetic energies. The absolute input energy is the work done by the total force applied to the base of the structure. The relative input energy is the work done by an equivalent lateral force on a fixed base system, and neglects the effects of rigid body translation (Uang and Bertero 1990).

Let  $V_{ea}$  and  $V_{er}$  be the maximum values of  $(2E_a/m)^{1/2}$  and  $(2E_r/m)^{1/2}$ , respectively. The energy-based velocities  $V_{ea}$  and  $V_{er}$  are asymptotic to the peak ground velocity for high and low oscillator frequencies, respectively.  $V_{ea}$  and  $V_{er}$  are nearly equivalent for oscillator frequencies within the band of appreciable PSV response, corresponding to that part of the Fourier spectrum of the ground acceleration with significant amplitudes. They diverge outside that frequency band. At oscillator frequencies low compared to the dominant frequencies of the ground acceleration,  $V_{ea}$  approaches zero, whereas  $V_{er}$  is asymptotic to the maximum ground velocity. At high oscillator frequencies,  $V_{er}$  approaches zero, whereas  $V_{ea}$  is asymptotic to the maximum ground velocity. Regardless of oscillator frequency,  $E_a = E_r$  if both are evaluated at the end of the ground motion episode. However, the maximum values of  $E_a$  and  $E_r$ , and the parameter  $V_{ea}$  of interest here, do not generally occur at the end of the ground motion episode. For example, in the case of high frequency oscillators,  $V_{ea}$  occurs near the time of the maximum ground velocity, and is larger than  $V_{er}$ .

Figure 2 illustrates the relationship between the energy parameters  $V_{ea}$ ,  $V_{er}$  and the PSV spectrum.

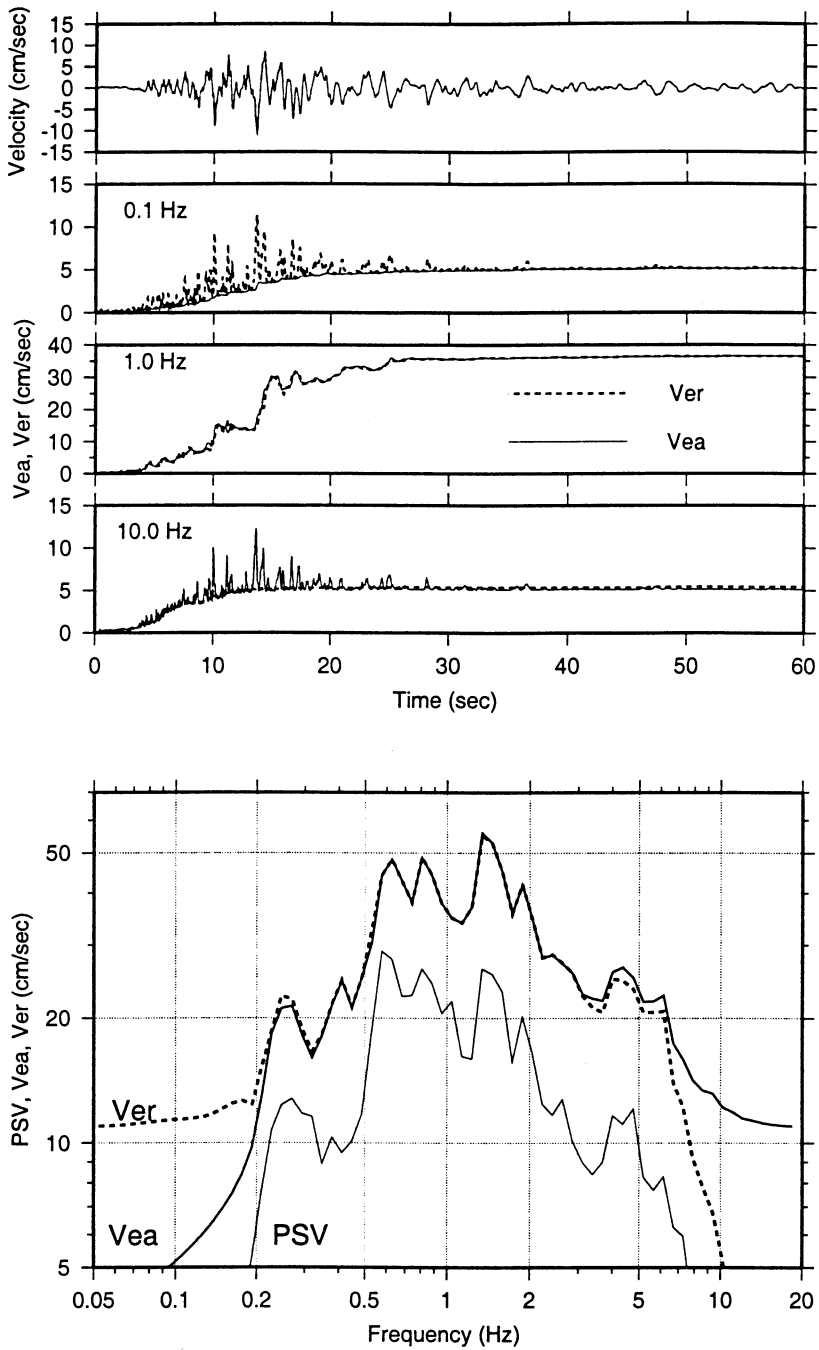


Figure 2. Relationships between  $PSV$  and energy-based velocities  $Vea$  and  $Ver$ , using the E-W component at Alhambra from the Northridge earthquake. Top: ground velocity. Middle:  $Vea$  and  $Ver$  for 5% damping, at frequencies 0.1, 1.0 and 10.0 Hz. Bottom:  $PSV$ ,  $Vea$  and  $Ver$  spectra.

### REGRESSION ANALYSIS

The following regression model (Boore et al. 1993) is fitted to the  $PSV$  and  $Vea$  data sets, and to the peak ground acceleration  $PGA$  and velocity  $PGV$  data.

$$\log_{10} Y = a + b(M-6) + c(M-6)^2 + d \log(r^2 + h^2)^{1/2} + e G_1 + f G_2 + \varepsilon. \quad (7)$$

Here,  $Y$  is the response variable (the geometric mean of the two horizontal components), expressed in units of centimeters and seconds,  $M$  is moment magnitude,  $r$  is the horizontal distance, in km, to the nearest surface projection of the fault rupture, and  $G_1$  and  $G_2$  are

indicator variables for site classifications  $C$  and  $D$  (e.g.:  $G_1=1$  for class C sites, 0 otherwise,  $G_2 = 1$  for class D sites, 0 otherwise). The unknowns  $a, b, c, d, h, e, f$  and the variance  $\sigma^2$  of random error  $\varepsilon$  are determined using the two-step regression procedure of Joyner and Boore (1993, 1994).

The normally distributed error term  $\varepsilon$  has zero mean and standard deviation  $\sigma$  composed of two components, such that  $\sigma^2 = \sigma_r^2 + \sigma_e^2$ . The variance  $\sigma_r^2$  is associated with the first stage of the regression wherein the unknowns  $d, h, e$  and  $f$  are estimated, along with "amplitude factors" for each of the earthquakes. The variance  $\sigma_e^2$  is that associated with the second stage regression wherein the amplitude factors are regressed against magnitude. For the model of a randomly oriented horizontal component, the response  $Y$  is the geometric mean of the two horizontal components, and the estimate of  $\sigma_r^2$  must be increased to account for the variance associated with choosing one of the components randomly (Boore et al. 1993).

### PEAK ACCELERATION, VELOCITY

To avoid bias due to non-triggered stations, the  $PGA$  regression model was developed iteratively, as described by Campbell (1997). In the first step, the entire assembled data set was used to determine a set of minimum distances at which the 16th percentile values of the model is less than  $0.02g$ , corresponding to a  $0.01g$  vertical component trigger threshold. These distances are functions of magnitude and site condition. Next, corresponding data points at larger distances were deleted and the regression was repeated. One iteration was sufficient to eliminate potentially biased data points, based on the 16th percentile criterion. Figure 3 plots the minimum cutoff distances as a function of magnitude and site class.

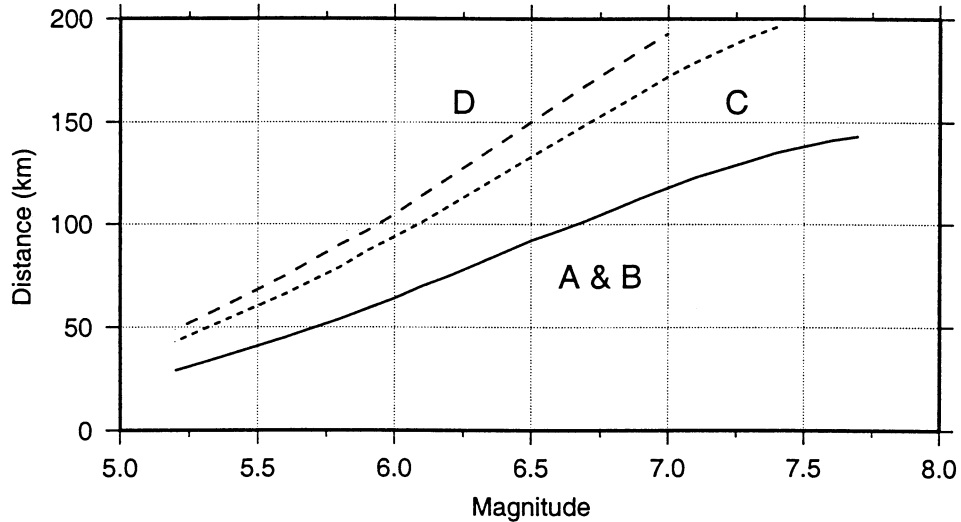


Figure 3. Data selection cutoff distance versus magnitude and site class.

Table A2 in the appendix lists the results of the regression analysis for peak ground acceleration  $PGA$  and velocity  $PGV$ . Figure 4 plots the models for the randomly oriented horizontal component, for the combined site classes A & B, as a function of magnitude and distance. Figures 5 and 6 show the regression residuals as functions of distance and magnitude. Figure 4 suggests that  $PGA$  undergoes saturation for  $M>6.5$ . Also, the effect of site classification is larger for  $PGV$  than for  $PGA$ . Regression coefficients  $e$  and  $f$  for  $PGA$  correspond to amplification factors of 1.40 and 1.55 for site classes C and D, respectively. These amplification factors have values of 1.53 and 2.00, respectively, for  $PGV$ . Figures 5

and 6 show that Equation 7 does a good job overall of fitting the  $PGA$  and  $PGV$  data, with no obvious non-normal magnitude or distance dependent trends apparent in the residual plots. The data scatter for  $PGV$  is somewhat larger than for  $PGA$ .

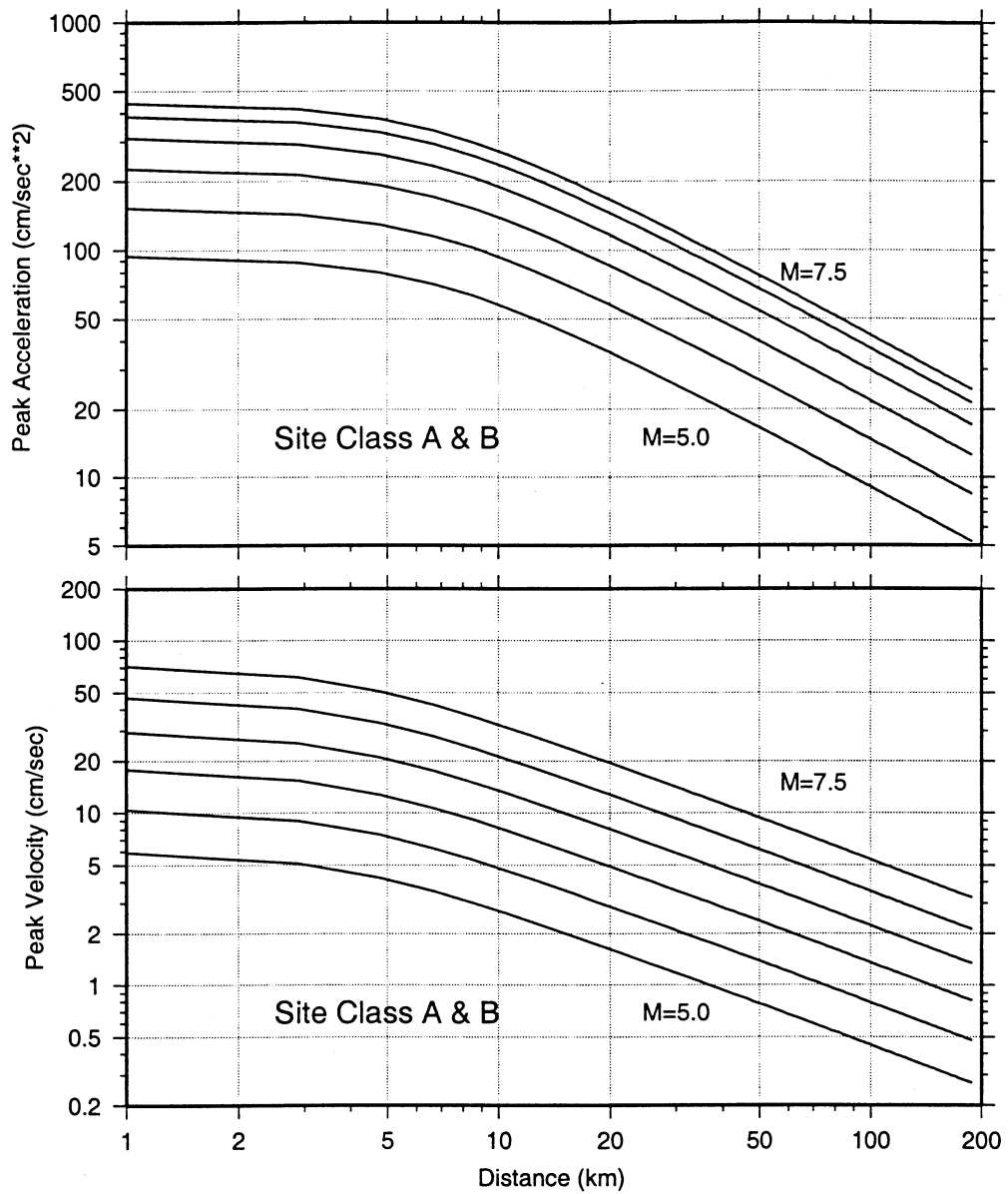


Figure 4. Top:  $PGA$  for a randomly oriented horizontal component. Curves are plotted for magnitudes 5.0, 5.5, 6.0, 6.5, 7.0 and 7.5. Site class C and D models exceed those plotted by factors of 1.40 and 1.55, respectively. Bottom:  $PGV$ . Site class C and D models exceed those plotted by factors 1.53 and 2.00, respectively.

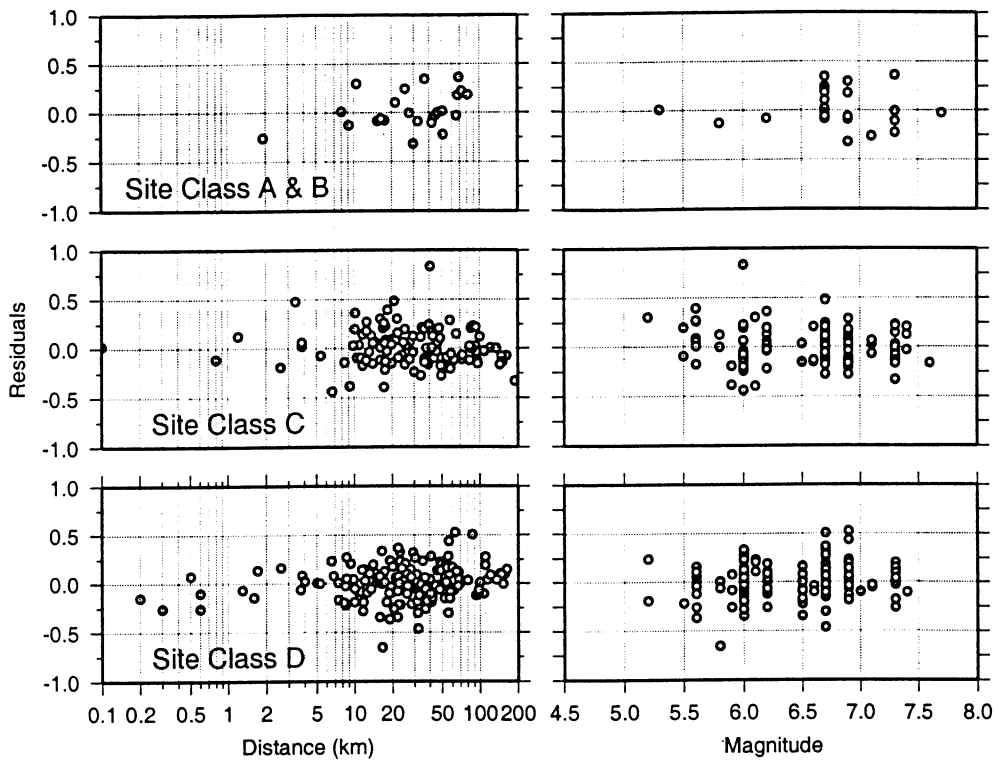


Figure 5. Regression residuals for  $PGA$ , randomly oriented horizontal component.

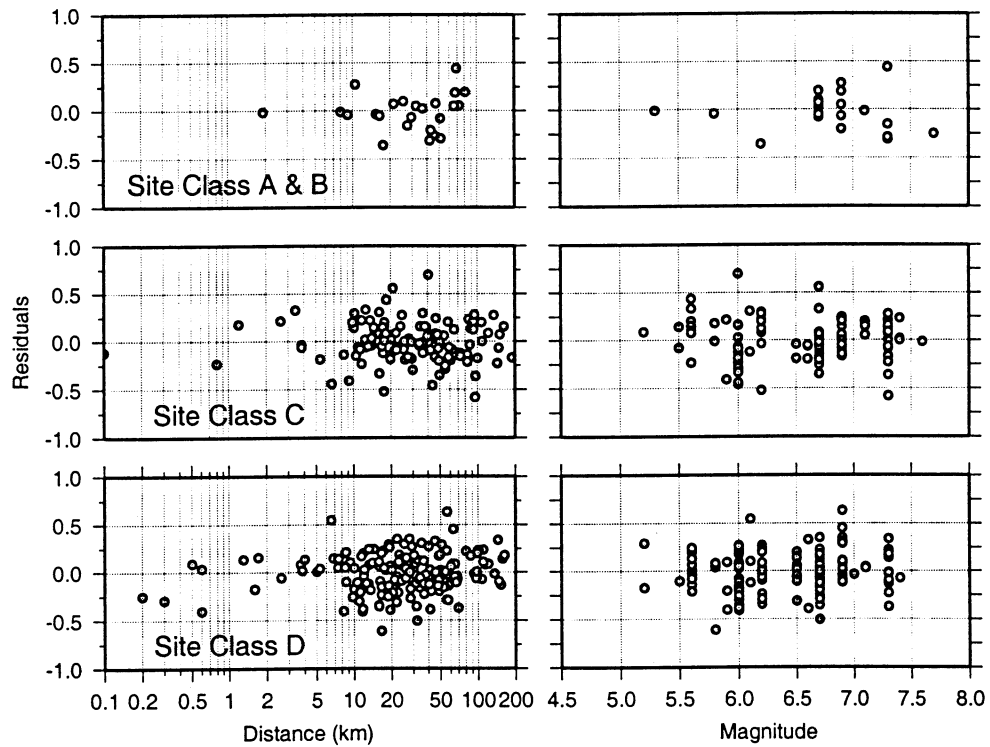


Figure 6. Regression residuals for  $PGV$ , randomly oriented horizontal component.

#### PSV AND ENERGY SPECTRA

Figure 7 compares the regression coefficients versus frequency for  $V_{ea}$  and  $PSV$  at 5% damping. The linear magnitude coefficient  $b$  is significantly larger (more positive) for the energy-based parameter  $V_{ea}$  than for  $PSV$ , at the higher frequencies, indicating a stronger high-

frequency scaling of  $V_{ea}$  with magnitude. The distance coefficient  $d$  is also more positive for  $V_{ea}$ , indicating a tendency for less distance attenuation of the parameter, compared to  $PSV$ , at all frequencies. The parameter  $h$ , which functions as a pseudo-focal depth term, is nearly the same for  $V_{ea}$  and  $PSV$  for frequencies less than about 3 Hz. At higher frequencies,  $h$  for  $PSV$  exceeds that for  $V_{ea}$ . The site class coefficients  $e$  and  $f$  are very similar for  $V_{ea}$  and  $PSV$ . In both cases, the effect of site class is most important at the lower frequencies. The effects of site class are unresolved by the regression analysis at frequencies greater than 5 Hz. Finally, the standard deviation of the regression,  $\sigma$ , generally decreases with increasing oscillator frequency, and is uniformly smaller for  $V_{ea}$  than for  $PSV$ . The results just described are much the same for the 2% and 10% damped oscillators.

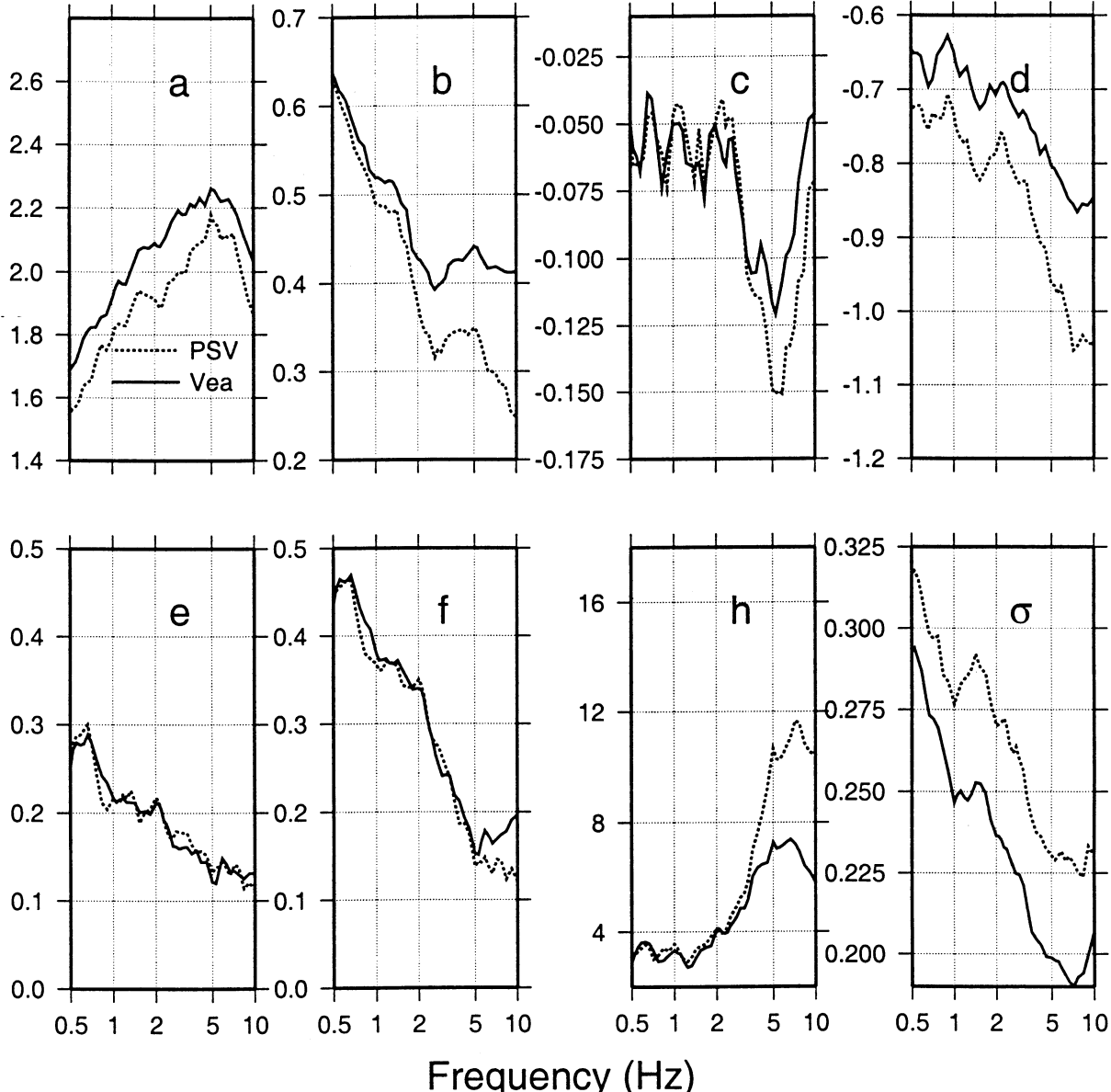


Figure 7. Estimated regression model coefficients for  $PSV$  and  $V_{ea}$ , as functions of oscillator frequency (5% damping).

The relative magnitude and distance dependence of  $PSV$  and  $V_{ea}$  is illustrated in figure 8 which plots the ratio  $V_{ea}/PSV$  derived from the regression models, versus distance for discrete

values of magnitude and oscillator frequency. The ratio  $V_{ea}/PSV$  is an increasing function of magnitude and distance, for distances greater than about 15 km. This means that  $V_{ea}$  increases more rapidly with increasing earthquake magnitude, and decays more slowly at larger distances. However, the effect is strongly dependent upon oscillator frequency. The difference between magnitude and distance scaling of  $V_{ea}$  and  $PSV$  is largest at the highest oscillator frequency (10 Hz), and is negligible for oscillator frequencies less than about 2 Hz.

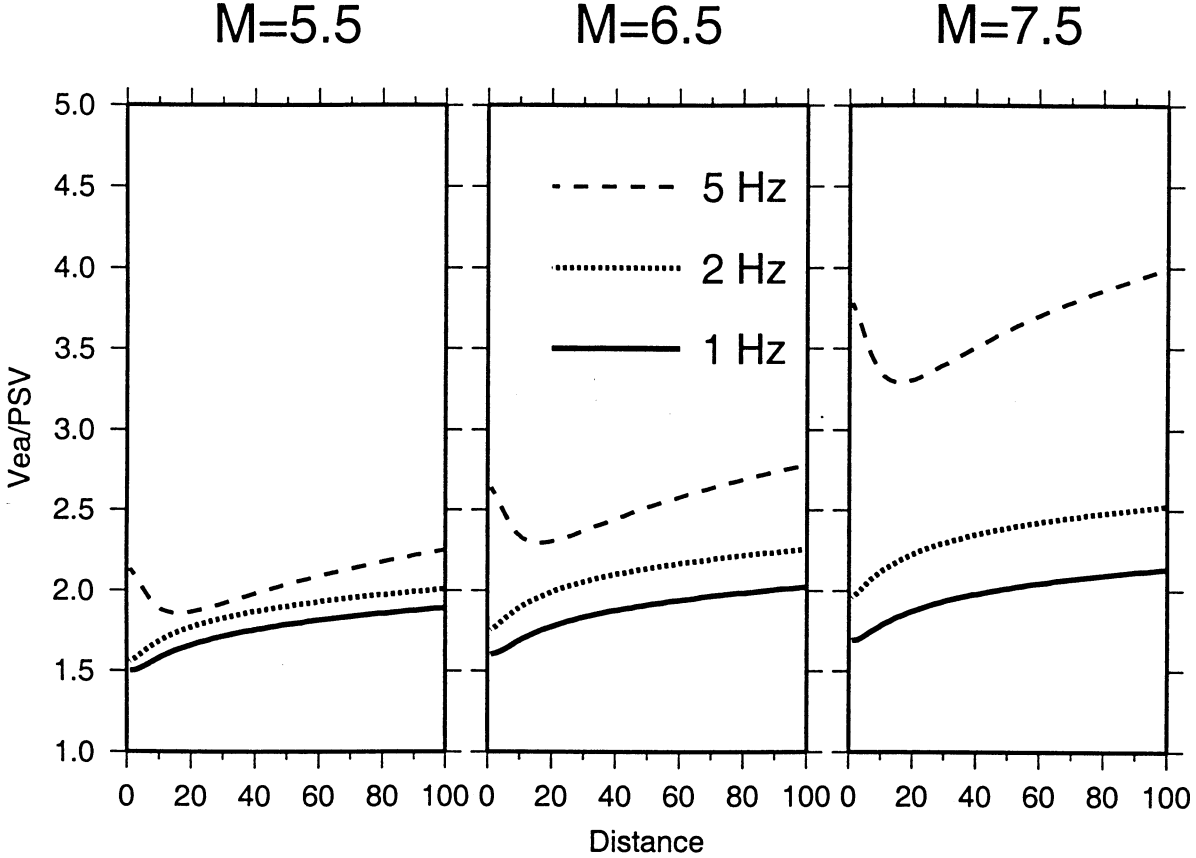


Figure 8. The ratio  $V_{ea}/PSV$  versus distance for  $M=5.5$  (left),  $M=6.5$  (center) and  $M=7.5$  (right). Results for 3 different oscillator frequencies are shown, for 5% damping and a randomly oriented horizontal component, site class A and B, combined.

Figure 9 summarizes some important differences between  $PSV$  and  $V_{ea}$ , by plotting both spectra for several magnitudes at 5 and 50 km distance. At low frequencies (less than approximately 2 Hz)  $V_{ea}$  and  $PSV$  spectra exhibit similar magnitude scaling. At the higher frequencies the  $PSV$  spectra exhibit near saturation for  $M>6.5$ , whereas the  $V_{ea}$  spectra continue to increase with increasing earthquake magnitude.

Tables A3 through A5 in the appendix list regression results for  $PSV$  for 3 values of damping (2%, 5% and 10% critical). Tables A6 through A8 list corresponding results for  $V_{ea}$ . Figure 10 shows  $PSV$  residuals versus distance and magnitude for 5 Hz oscillators. Figure 11 shows corresponding residual plots for  $V_{ea}$ . The residual plots for other oscillator frequencies are similar to those shown, with no obvious magnitude or distance dependent trends: however, variance increases systematically with decreasing frequency. The regression model is equally appropriate for  $PSV$  and  $V_{ea}$ .

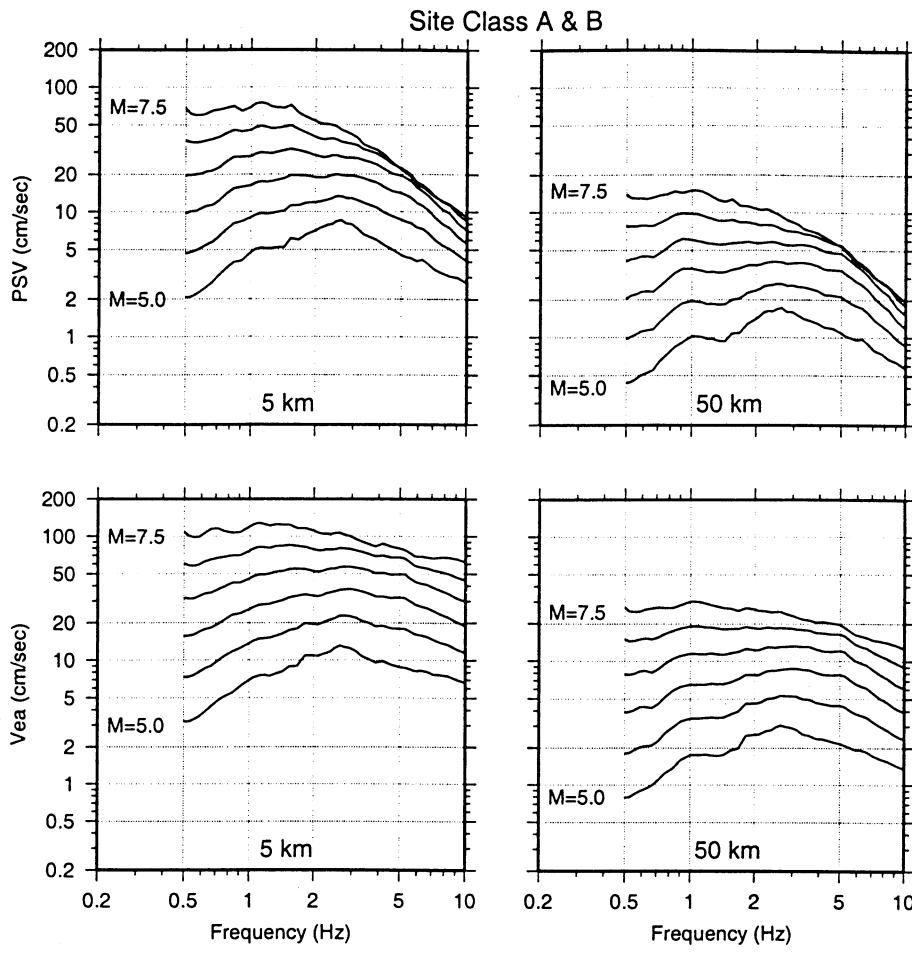


Figure 9. PSV (upper) and Vea (lower) spectra for site class A and B, combined. Spectra are for 5% damping, and a randomly oriented horizontal component, for 5 and 50 km distances.

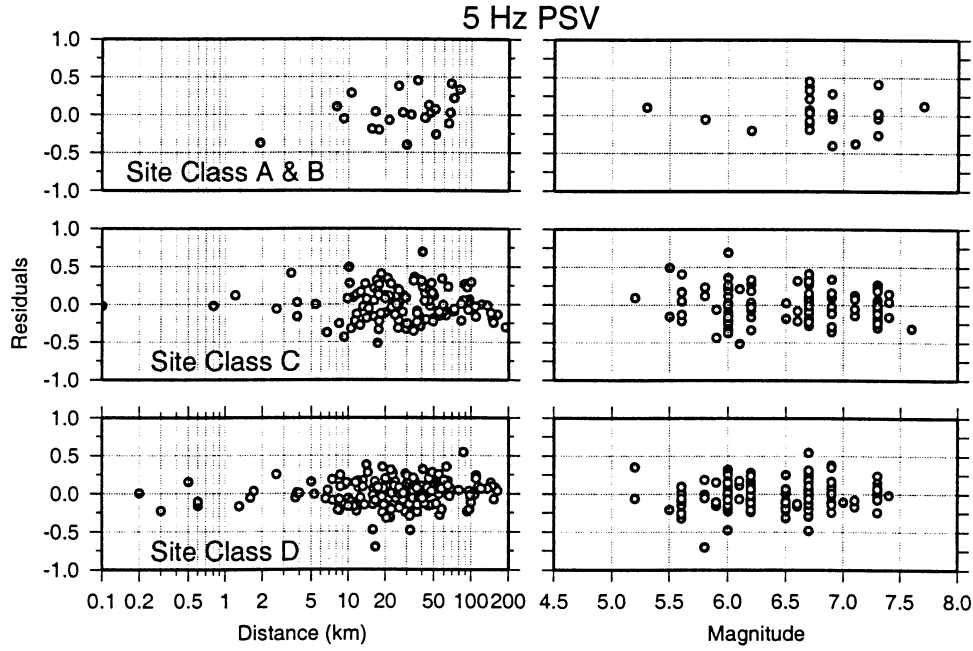


Figure 10. PSV regression residuals for 5 Hz oscillators, 5% damping, randomly oriented horizontal component.

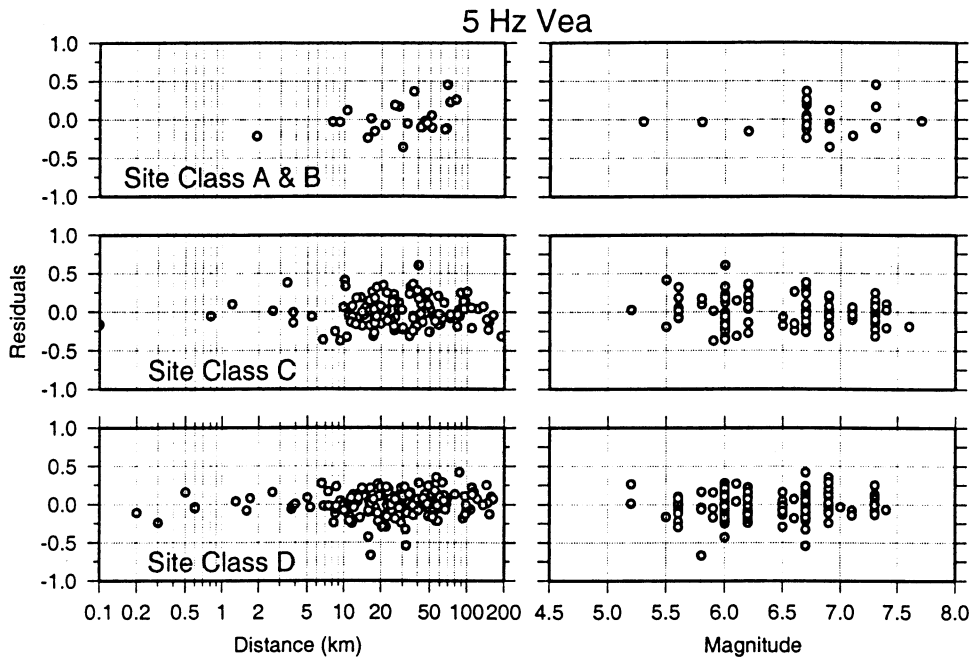


Figure 11. *Vea* regression residuals for 5 Hz oscillators, 5% damping, randomly oriented horizontal component.

### IMPLICATIONS FOR SEISMIC HAZARD ASSESSMENT

The identification of the events, in terms of magnitude and distance, that contribute most to seismic hazard for a given probability of exceedance has practical application. It can serve as a guide for defining scenarios and design earthquakes for engineering problems, particularly those involving dynamic analysis using ground motion time series. In the following, we examine differences in the results of simple hazard calculations using the two different motion parameters.

For simplicity, assume a hazard model wherein the random variables are statistically independent and limited to those appearing in the motion prediction model ( $M$ ,  $r$  and  $\varepsilon$ , Equation 7). For convenience,  $\varepsilon$  will be treated below as a standardized normally distributed variable. For these assumptions, the seismic hazard from a single source can be represented (McGuire 1995) as

$$E(x) = \iiint v f_M(m) f_R(r) f_E(\varepsilon) H[Y(m, r, \varepsilon) - \log x] dm dr d\varepsilon, \quad (8)$$

where  $E(x)$  is the expected rate of exceeding motion parameter value  $x$ . The rate of earthquakes in the source is  $v$ . The probability densities of the random variables  $M$ ,  $r$  and  $\varepsilon$  are  $f_M(m)$ ,  $f_R(r)$  and  $f_E(\varepsilon)$ ;  $H$  is the Heaviside function, and  $Y(m, r, \varepsilon)$  is the motion prediction model. The limits of integration depend upon the geometry of the source, the maximum potential magnitude of the source and the distribution function of the random error.

Let  $U(m, r, \varepsilon | x)$  represent the integrand of (8), for a specific value of  $x$ . This value  $x$  could correspond to some chosen hazard value  $E(x)$  of say, 1/1000 (1000 year return period). Let  $(\underline{m}, \underline{r}, \underline{\varepsilon})$  define the location of the maximum value of  $U(m, r, \varepsilon | x)$ . This is the "β-point" (McGuire 1995) and is the modal value of the joint distribution of the random variables for the selected hazard value  $E(x)$ . A marginal distribution  $U'(m, r | x)$  can be obtained by integration of  $U(m, r, \varepsilon | x)$  with respect to standardized variable  $\varepsilon$ . Let the maximum value of

$U'(m, r | x)$  occur at  $(\underline{m}', \underline{r}')$ . In general,  $\underline{m}$  and  $\underline{r}$  are not equivalent to  $\underline{m}'$  and  $\underline{r}'$ .

We will compare results using  $V_{ea}$  and  $PSV$  for the general (elemental) model of a point source for earthquakes. We assume the following recurrence model:  $\log N = 2.8 - 0.8 M$ . We assume a truncated exponential form for  $f_M(m)$ , with lower and upper magnitude bounds at  $M=5.0$  and  $M=7.7$ , and  $v = 0.0626$  events/year.

Figure 12 shows the marginal density functions  $U'(m, r | x)$  for several frequencies, for two cases: point sources at 10 and 60 km, and return periods 2500 and 500 years, respectively. As expected from the similarity of magnitude scaling in the regression models, there is little difference in the density functions for the low frequency oscillators (e.g., 0.5 and 1.0 Hz). For 2.0 Hz,  $\underline{m}'$  for  $V_{ea}$  is approximately 0.2 magnitude units larger than  $\underline{m}'$  for  $PSV$ . This difference increases to approximately 0.6 units for the 6.7 Hz oscillator. Similar differences occur for  $\underline{m}$ . Table 2 summarizes the values of  $x$ ,  $(\underline{m}', \underline{r}')$  and the  $\beta$ -point  $(\underline{m}, \underline{r}, \underline{\varepsilon})$  for the examples shown in Figure 12. It is apparent that differences in magnitude scaling of  $V_{ea}$  and

Table 2. Modal events for the point source PSHA calculation

PSV					$V_{ea}$				
$P(X > x) = 1/2,500, 60 \text{ km}$									
Freq.	x	$\underline{m}'$	$\underline{m}$	$\underline{\varepsilon}$	x	$\underline{m}'$	$\underline{m}$	$\underline{\varepsilon}$	
0.5	16.7	7.46	7.08	1.12	30.6	7.46	7.03	1.20	
1.0	19.0	7.30	7.03	1.24	34.1	7.46	6.97	1.28	
2.0	15.8	7.03	6.70	1.68	31.8	7.30	7.03	1.24	
3.0	13.8	6.70	6.54	1.80	29.8	7.03	6.86	1.40	
4.0	10.8	6.59	6.50	1.80	25.5	7.03	6.86	1.40	
5.0	9.9	6.49	6.43	1.80	24.8	6.97	6.81	1.44	
6.7	6.6	6.38	6.27	1.96	18.5	7.03	6.92	1.32	
$P(X > x) = 1/500, 10 \text{ km}$									
Freq.	x	$\underline{m}'$	$\underline{m}$	$\underline{\varepsilon}$	x	$\underline{m}'$	$\underline{m}$	$\underline{\varepsilon}$	
0.5	24.9	6.86	6.49	1.00	40.0	6.86	6.54	0.88	
1.0	33.5	6.70	6.38	1.16	52.6	6.86	6.54	0.88	
2.0	34.0	6.54	6.22	1.36	59.1	6.76	6.32	1.24	
3.0	32.7	6.32	6.11	1.44	61.0	6.59	6.27	1.28	
4.0	27.1	6.27	6.16	1.32	55.1	6.65	6.43	1.00	
5.0	24.8	6.27	6.16	1.28	54.2	6.65	6.32	1.16	
6.7	17.8	6.16	6.00	1.48	43.6	6.65	6.43	1.00	

$PSV$  result in substantial differences of the derived modal earthquake magnitudes of the  $U$  and  $U'$  density distributions, at higher frequencies. The modal magnitudes for  $V_{ea}$  (either  $\underline{m}'$  or  $\underline{m}$ ) are larger than those for  $PSV$ , and tend to decrease less rapidly (i.e., vary less) with increasing oscillator frequency. In this example, scenarios based on  $\underline{m}$  would, in the case of  $V_{ea}$ , focus on earthquakes with magnitudes in the relatively narrow range 6.81 to 7.03 for the 60 km,

2500 year scenario, whereas if the calculations are done using  $PSV$ , a much wider range

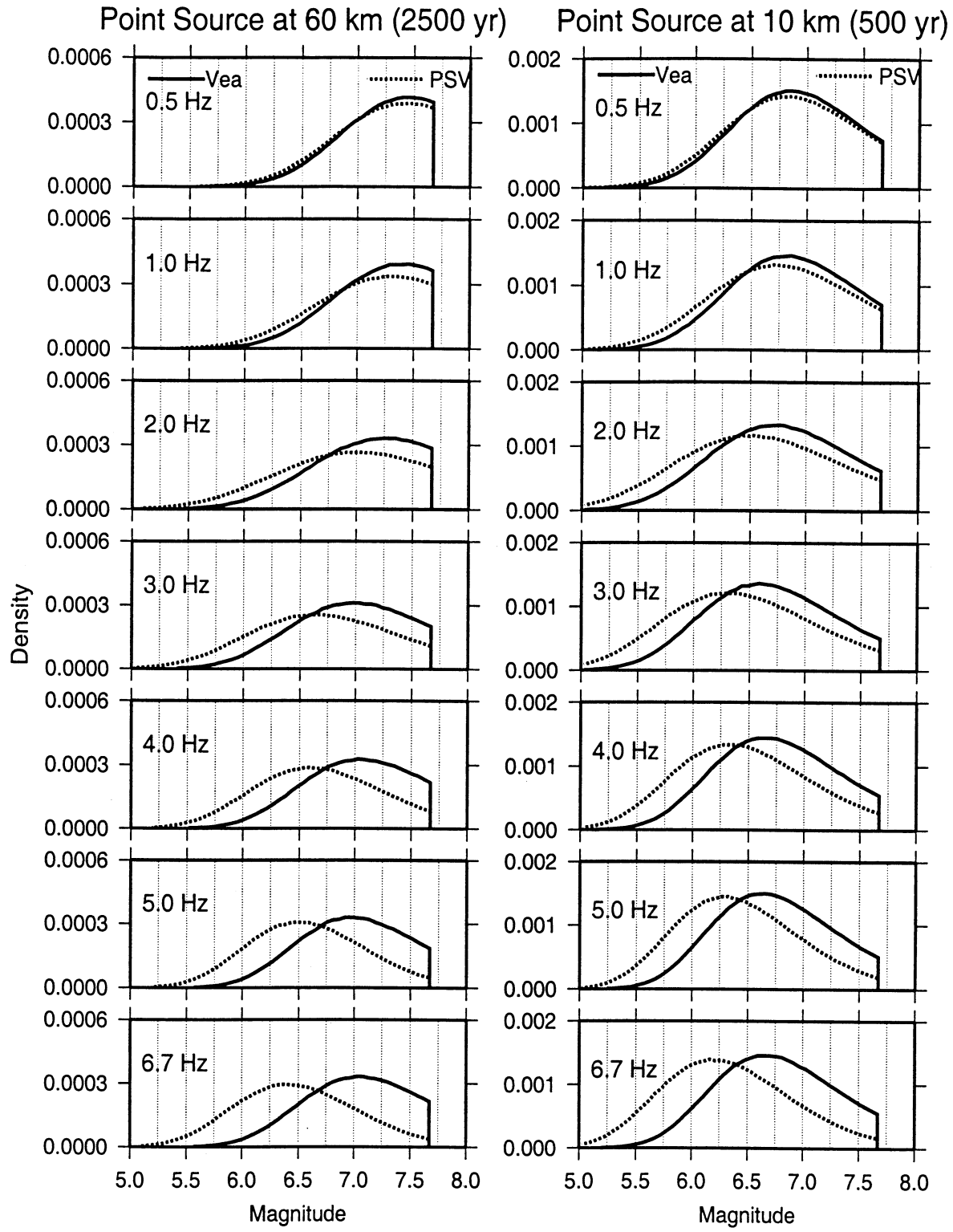


Figure 12. Marginal density functions  $U'$  for two examples involving point sources for earthquakes at 60 km (left) and 10 km (right). Refer to Table 2 for values of the modal magnitudes and motion values.

of magnitudes (6.27 to 7.08) is indicated for the frequency band 0.5 to 6.67 Hz. Clearly, the choice of motion parameter has a substantial impact upon the perceived source of the seismic hazard. This has implications for the problem of design earthquake selection. In this simple

example, use of  $V_{ea}$  puts more emphasis upon a scenario involving a larger magnitude shock, than would be the case if  $PSV$  where used in the hazard calculation.

## CONCLUSIONS

The study examines the use of the elastic input energy spectrum as a basis for seismic hazard calculations, using strong motion data from Western North America. Regression modeling using consistent processing procedures for the elastic absolute input energy equivalent velocity  $V_{ea}$ , and the elastic response  $PSV$  in the frequency range 0.5 to 10 Hz shows that the two parameters can be successfully fit with identical functional forms. The variance of  $V_{ea}$  is uniformly less than that of  $PSV$ , indicating that  $V_{ea}$  can be predicted with slightly less uncertainty, as a function of magnitude, distance and site classification. The dependence of  $V_{ea}$  and  $PSV$  upon NEHRP site classification (BSSC, 1994) is virtually identical. The effects of site class are important at frequencies less than a few Hertz. The regression modeling does not resolve significant effects due to site class at frequencies greater than approximately 5 Hz.

The elastic input energy offers a potential advantage over the elastic response spectrum in that it reflects, by integration, the effect of ground motion duration. This is evident in the regression models by a stronger magnitude scaling of  $V_{ea}$ , compared to  $PSV$ , for oscillator frequencies greater than approximately 2 Hz. The implication for probabilistic hazard analysis is that if the hazard is assessed on the basis of  $V_{ea}$ , the hazard posed by the larger magnitude earthquakes contributes more to the total hazard, than would be the case if the assessment where done on the basis of the elastic response spectrum. Disaggregation of point source seismic hazard models using  $V_{ea}$  indicates that the modal magnitudes for the higher frequency oscillators tend to be larger, and vary less with oscillator frequency, than those derived using  $PSV$ . These results will hold in general for more complicated seismic hazard models. The elastic input energy is a convenient parameter that captures both amplitude and duration characteristics of the ground motion time series. Its use in probabilistic seismic hazard analysis could provide an improved basis for selecting earthquake scenarios when duration of shaking is a design consideration.

## ACKNOWLEDGMENTS

This study was supported by the U. S. Geological Survey through contract number 1434-HQ-97-GR-03067. I thank W. B. Joyner and D. M. Boore for guidance and assistance. The Generic Mapping Tools software (Wessel and Smith, 1991) was used to prepare the figures.

## APPENDIX

Table A1. Strong Motion Recordings Used in Regression Analysis

Site Name	Site Number*	Az1	Az2	Dist (km)	Lat. N	Lon. W	Class
<i>Imperial Valley, May 19, 1940, M=7.0</i>							
El Centro #9	(ct 117)	180	270	12.0	32.795	115.549	c
<i>Kern County, July 21, 1952, M=7.4</i>							

Site Name	Site Number*	(ct 95)	21	111	42.0	35.150	119.450	b
		Az1	Az2		Dist (km)	Lat. N	Lon. W	Class
Santa Barbara CH	(ct 283)	42	132	85.0	34.424	119.701	b	
Cal Tech Athena.	(ct 475)	180	270	109.0	34.139	118.121	b	
Hollywood St. Bld.	(ct 135)	180	90	107.0	34.083	118.333	c	
<b>Daly City, March 22, 1957, M=5.3</b>								
Golden Gate Park	(ct 077)	10	100	8.0	37.667	122.483	a	
<b>Parkfield, June 28, 1966, M=6.6</b>								
Cholame Shandon #2	(ct 13)	65	---	6.6	35.731	120.286	c	
Cholame Shandon #5	(ct 14)	355	85	9.3	35.700	120.328	c	
Cholame Shandon #8	(ct 15)	50	320	13.0	35.671	120.360	c	
Cholame Shandon #12	(ct 16)	50	320	17.3	35.636	120.403	b	
Cholame Shandon Tmblor #2	(ct 97)	295	205	16.1	35.752	120.264	b	
<b>Borrego Mtn., April 9, 1968, M=6.6</b>								
El Centro Array #9	(ct 117)	90	270	45.0	32.794	115.54	c	
<b>San Fernando, Feb. 9, 1971, M=6.6</b>								
Caltech Athenaeum	(ct 475)	0	90	25.7	34.139	118.121	b	
Lake Hughes Sta. 4	(ct 126)	111	201	19.6	34.642	118.480	c	
Lake Hughes Sta. 12	(ct 128)	21	249	17.0	34.572	118.560	b	
Wrightwood	(ct 290)	25	115	60.7	34.361	117.633	b	
<b>Sitka, July 30, 1972, M=7.7</b>								
Sitka magnetic observatory	(2714)	180	90	45.0	57.060	135.320	a	
<b>Managua, Dec., 23, 1972, M=6.2</b>								
ESSO Refinery	----	180	90	5.0	12.145	86.322	c	
<b>Hollister, Nov. 28, 1974, M=5.2</b>								
San Juan Batista	---	237	33	10.0	36.860	121.540	c	
Hollister City Hall annex	(usgs 1575)	181	271	19.0	36.851	121.402	c	
Gilroy -Gavilan College	(cdmg 47379)	247	157	22.0	36.973	121.572	b	
<b>St. Elias, Feb. 28, 1979, M=7.6</b>								
Icy Bay, Gulf Timber Co.	(2734)	180	90	25.4	59.968	141.643	b	
<b>Coyote Lake, Aug. 6, 1979, M=5.8</b>								
Gilroy Array 1	(cdmg 47379)	320	230	9.1	36.973	121.572	a	
Gilroy Array 2	(cdmg 47380)	140	50	7.4	36.982	121.556	c	
Gilroy Array 3	(cdmg 47381)	140	50	5.3	36.987	121.536	c	
Gilroy Array 4	(cdmg 57382)	360	270	3.7	36.005	121.522	c	
Gilroy Array 6	(cdmg 57383)	320	230	1.2	37.026	121.484	b	
<b>Imperial Valley, Oct. 15, 1979, M=6.5</b>								
El Centro Array #7	(usgs 5028)	230	140	0.6	32.829	115.504	c	
El Centro Array #6	(usgs 5158)	230	140	1.3	32.839	115.487	c	
El Centro Bonds Corner	(usgs 5054)	230	140	2.6	32.693	115.338	c	
El Centro Array #8	--	230	140	3.8	32.810	115.530	c	

El Centro Array #5  
Table A1 (cont.)

(usgs 0952) 230 140 4.0 32.855 115.466 c

Site Name		Site Number*	Az1	Az2	Dist (km)	Lat. N	Lon. W	Class
El Centro Array #4	(usgs 0955)	230	140	6.8	32.864	115.432	c	
Brawley	(usgs 5060)	315	225	8.5	32.991	115.512	c	
El Centro Array #10	(usgs 0412)	50	320	8.5	32.780	115.567	c	
Parachute Test Site	(usgs 5051)	315	225	14.0	32.929	115.699	b	
El Centro Array #2	(usgs 5115)	230	140	16.0	32.916	115.366	c	
El Centro Array #12	(usgs 0931)	230	140	18.0	32.718	115.637	c	
Calipatria	(usgs 5061)	315	225	23.0	33.130	115.520	c	
El Centro Array #13	(usgs 5059)	230	140	22.0	32.709	115.683	c	
El Centro Array #1	(usgs 5056)	230	140	22.0	32.960	115.319	c	
Superstition Mtn	(usgs 0286)	135	45	26.0	32.955	115.823	b	
Holtville	(usgs 5055)	315	225	7.5	32.812	115.377	c	
Calexico	(usgs 5053)	315	225	10.6	32.669	115.492	c	

Livermore, Jan. 24, 1980, M=5.9

San Ramon	(cdmg 0134)	70	340	16.7	37.780	121.980	c
APEEL 3E	(cdmg 0219)	146	236	40.3	37.656	122.060	b

Livermore, Jan. 27, 1980, M=5.2

San Ramon	(cdmg 0134)	70	340	22.5	37.780	121.980	c
APEEL 3E	(cdmg 0219)	236	146	37.8	37.656	122.060	b
Morgan Territ. Pk, Livermore	(cdmg 0000)	355	265	10.1	37.818	121.795	b

Westmoreland, April 26, 1981, M=5.6

Brawley Airport	(usgs 5060)	135	225	11.2	32.990	115.510	c
Parachute Test Site	(usgs 5247)	315	225	2.6	32.930	115.700	b
Salton Sea Wildlife Refuge	(usgs 5062)	315	225	0.6	33.180	115.620	c
Superstition Mtn	(usgs 286)	135	45	9.2	32.950	115.820	b
Westmoreland	(cdmg 11369)	90	180	0.5	33.037	115.623	c

Morgan Hill, April 24, 1984, M=6.2

Anderson Dam (downstream)	(usgs 1652)	340	250	3.8	37.165	121.631	b
Gilroy #1	(cdmg 47379)	67	337	17.6	36.973	121.572	a
Gilroy #2	(cdmg 47380)	90	0	16.6	36.982	121.556	c
Gilroy #4	(cdmg 57382)	360	270	14.5	37.005	121.522	c
Gilroy #6	(cdmg 57383)	90	0	13.6	37.026	121.484	b
Gilroy #7	(cdmg 57425)	0	--	15.8	37.033	121.434	c
Halls Valley	(cdmg 57191)	240	150	0.3	37.338	121.714	c
Hollister Airport diff. array	(usgs 1656)	255	165	30.1	36.888	121.413	c
Gilroy #3	(cdmg 47381)	90	0	16.2	36.987	121.536	c
Gilroy, Gavilan College	(cdmg 47006)	67	23	17.6	36.973	121.568	b

Whittier, Oct. 1, 1987, M=6.0

Alhambra-Fremont sch.	(cdmg 24461)	270	180	3.8	34.070	118.150	b
LA Country Club North	(cdmg 24389)	90	0	28.5	34.063	118.418	c
LA Country Club South	(cdmg 24390)	90	0	28.3	34.062	118.416	c
LA Hollywd Storage bld. ff	(cdmg 24303)	90	0	21.2	34.090	118.339	c
Lake Hughes #1	(cdmg 24271)	90	0	72.3	34.674	118.430	b
Rancho Cucamonga - L&J	(cdmg 23497)	90	0	43.2	34.104	117.574	b
Sylmar	(cdmg 24514)	90	0	41.5	34.326	118.444	c
Tarzana	(cdmg 24436)	90	0	40.3	34.160	118.534	b
17645 Saticoy St., Northridge	(usc 03)	180	90	40.4	34.209	118.517	c

Site Name	Site Number*	Az1	Az2	Dist (km)	Lat. N	Lon. W	Class
9210 Sunland Blvd., Sun Valley	(usc 08)	310	220	29.6	34.235	118.367	b
Coldwater Cany. , Studio City	(usc 10)	182	92	29.1	34.146	118.413	c
542 N. Buena vista St., Burbank	(usc 12)	340	250	23.0	34.168	118.332	c
Mulholland Dr., Beverly Hills	(usc 13)	9	279	31.1	34.132	118.439	c
Mulholland Dr., Beverly Hills	(usc 14)	122	32	27.9	34.127	118.405	b
700 N. Faring Rd., LA	(usc 16)	90	0	30.1	34.089	118.435	b
600 E. Grand Ave., San Gabriel	(usc 19)	270	180	0.8	34.091	118.093	b
4312 S. Grand Ave., LA	(usc 22)	180	90	16.7	34.005	118.279	c
2369 E. Vernon Ave., LA	(usc 25)	173	83	12.6	34.004	118.230	c
5921 N. Figueroa St., LA	(usc 32)	58	328	8.4	34.111	118.189	b
624 Cypress Ave., LA	(usc 33)	143	53	10.5	34.088	118.222	b
3035 Fletcher Dr., LA	(usc 34)	234	144	13.2	34.115	118.244	c
Sunset Blvd., Pacific Palisades	(usc 49)	280	190	41.1	34.042	118.554	c
Pacific Coast Hyw., Malibu	(usc 51)	150	60	62.7	34.024	118.787	b
Las Virgenes Rd., Calabasas	(usc 52)	290	200	54.8	34.151	118.696	b
Lst. Can. Rd., Canyon Country	(usc 57)	0	270	48.0	34.419	118.426	c
New York Ave., La Crescenta	(usc 60)	180	90	22.4	34.238	118.253	c
Big Tujunga Station	(usc 61)	352	262	25.4	34.286	118.225	b
Angeles Nat. For., Mill Creek	(usc 62)	90	0	33.9	34.390	118.079	c
Las Palmas Ave., Glendale	(usc 63)	267	177	17.8	34.200	118.231	b
120 N. Oakbank, Glendora	(usc 65)	170	80	16.2	34.137	117.882	b
656 S. Grand Ave., Covina	(usc 68)	105	15	15.8	34.078	117.870	c
Holly Ave., Baldwin Park	(usc 69)	270	180	6.7	34.100	117.974	b
1271 W. Badillo, Covina	(usc 70)	0	270	11.7	34.087	117.915	c
1307 S. Orange, West Covina	(usc 71)	315	225	8.2	34.064	117.952	c
504 Rimgrove Ave., La Puente	(usc 72)	105	15	11.8	34.026	117.918	c
Colima Rd., Hacienda Heights	(usc 73)	230	140	11.0	33.990	117.942	c
950 Briarcliff Dr., La Habra	(usc 74)	90	0	13.5	33.921	117.972	c
E. Joslin St., Sante Fe Springs	(usc 77)	48	318	8.6	33.944	118.087	c
Castlegate St., Compton	(uscs78)	0	270	16.5	33.899	118.196	c
12500 Birchdale, Downey	(usc 79)	180	90	11.9	33.920	118.137	c
6979 Orange Ave., Long Beach	(usc 80)	10	280	17.3	33.881	118.176	c
21288 Water St., Carson	(usc 81)	270	180	24.5	33.836	118.239	c
6701 Del Amo, Lakewood	(usc 84)	90	0	19.4	33.846	118.099	c
5360 Saturn St., LA	(usc 91)	110	20	22.7	34.046	118.355	c
180 Campus Dr., Arcadia	(usc 93)	9	279	5.4	34.130	118.036	b
7420 Jaboneria, Bell Gardens	(usc 94)	297	207	8.5	33.965	118.158	c
1488 Old House Rd., Pasadena	(usc 95)	90	0	9.7	34.171	118.079	c

***Loma Prieta, Oct. 18, 1989, M=6.9***

Anderson Dam: Downstream	(usgs 1652)	340	250	20.0	37.166	121.628	b
Hollister Airport Diff Array	(usgs 1656)	255	165	25.4	36.888	121.413	c
Hollister City Hall Annex	(usgs 1575)	180	90	27.8	36.851	121.402	c
Stanford SLAC Test lab	(usgs 1601)	360	270	35.0	37.419	122.205	c
Hayward City Hall N. FF	(usgs 1129)	64	334	58.7	37.679	122.082	b
APEEL station 9	(usgs 1161)	227	137	46.4	37.478	122.321	b
Bear Valley sta. 5	(usgs 1474)	310	220	53.7	36.673	121.195	b
Bear Valley sta. 10	(usgs 1479)	310	220	67.3	36.532	121.143	c
Bear Valley sta. 12	(usgs 1481)	310	220	50.9	36.658	121.249	c
Calaveras Res. South gnd.	(usgs 1687)	180	90	36.1	37.452	121.807	b
Cherry Flat Reservoir	(usgs 1696)	360	270	32.5	37.396	121.756	a
Dublin Fire Station	(usgs 1689)	360	270	61.6	37.709	121.932	c

Hollister Sago Vault  
Table A1 (cont.)

(usgs 1032) 360 270 29.9 36.765 121.446 a

Site Name		Site Number*	Az1	Az2	Dist (km)	Lat. N	Lon. W	Class
Sunol Fire Station	(usgs 1688)	180	90	49.9	37.597	121.880	b	
Agnew	(cdmg 57066)	90	0	27.0	37.397	121.952	c	
Gilroy # 1	(cdmg 47379)	90	0	10.5	36.973	121.572	a	
Monterey city hall	(cdmg 47377)	90	0	42.7	36.597	121.897	a	
San Fran. Sierra Point	(cdmg 58539)	205	115	67.6	37.674	122.388	a	
Corralitos	(cdmg 57007)	90	0	0.1	37.046	121.803	b	
Gilroy #1 Gavilan College	(cdmg 47006)	67	337	10.9	36.973	121.568	b	
Saratoga	(cdmg 58065)	90	0	11.7	37.255	122.031	b	
Santa Cruz	(cdmg 58135)	90	0	12.5	37.001	122.060	b	
San Jose: Santa Teresa Hills	(cdmg 57563)	225	315	13.2	37.210	121.803	b	
Gilroy #6	(cdmg 57383)	90	0	19.9	37.026	121.484	b	
SAGO south	(cdmg 47189)	351	261	34.1	36.753	121.396	b	
Woodside	(cdmg 58127)	90	0	38.7	37.429	122.258	b	
Hayward BART FF	(cdmg 58498)	310	220	57.7	37.670	122.086	b	
Capitola	(cdmg 47125)	90	0	8.6	36.974	121.952	c	
Gilroy #2	(cdmg 47380)	90	0	12.1	36.982	121.556	c	
Gilroy #3	(cdmg 47381)	90	0	14.0	36.987	121.536	c	
Gilroy #4	(cdmg 57382)	90	0	15.8	37.005	121.522	c	
Gilroy #7	(cdmg 57425)	90	0	24.3	37.033	121.434	c	
Halls Valley	(cdmg 57191)	90	0	29.3	37.338	121.714	c	
Salinas	(cdmg 47179)	250	160	31.4	36.671	121.642	c	
Fremont	(cdmg 57064)	90	0	42.4	37.535	121.929	c	
San Fran. Airport	(cdmg 58223)	90	0	63.2	37.622	122.398	c	

***Sierra Madre, June 28, 1991, M=5.6***

17645 Saticoy St., Northridge	(usc 03)	180	90	44.0	34.209	118.517	c
600 E. Grand Ave., San Gabriel	(usc 19)	270	180	17.7	34.091	118.093	b
3035 Fletcher Dr., LA	(usc 34)	234	144	23.8	34.115	118.244	c
Canoga Park	(usc 53)	196	106	52.1	34.212	118.606	c
Lst. Can. Rd., Canyon Country	(usc 57)	0	270	39.9	34.419	118.426	c
New York Ave., La Crescenta	(usc 60)	180	90	19.6	34.238	118.254	c
Big Tujunga Station	(usc 61)	352	262	17.3	34.286	118.225	b
Las Palmas Ave., Glendale	(usc 63)	267	177	18.4	34.200	118.231	b
120 N. Oakbank, Glendora	(usc 65)	170	80	14.8	34.137	117.883	b
11338 Fariview Ave., El Monte	(usc 66)	185	95	16.7	34.093	118.019	c
237 Mel Canyon Rd., Duarte	(usc 67)	180	90	11.6	34.150	117.939	b
Holly Ave., Baldwin Park	(usc 69)	270	180	16.1	34.100	117.974	b
1271 W. Badillo, Covina	(usc 70)	0	270	18.9	34.087	117.915	c
1307 S. Orange, West Covina	(usc 71)	315	225	20.4	34.064	117.952	c
E. Joslin St., Sante Fe Springs	(usc 77)	48	318	33.5	33.944	118.087	c
180 Campus Dr., Arcadia	(usc 93)	9	279	12.6	34.130	118.036	b
7420 Jaboneria, Bell Gardens	(usc 94)	310	220	32.8	33.965	118.158	c
855 Arcadia Ave., Arcadia	(usc 99)	262	172	13.1	34.127	118.059	c

***Petrolia, April 25, 1992, M=7.1***

Ferndale Fire Sta	(usgs 1023)	360	270	10.0	40.576	124.262	c
Loleta Fire Sta	(usgs 1586)	360	270	17.6	40.644	124.219	b
Centerville Beach	(usgs 1585)	360	270	9.8	40.563	124.348	b
College of Redwood	(usgs 1582)	360	270	23.9	40.699	124.200	b
South Bay school	(usgs 1581)	360	270	27.8	40.735	124.207	c
Fortuna Fire Sta	(usgs 1583)	360	270	14.6	40.599	124.154	b
Bunker Hill FAA	(usgs 1584)	360	270	1.9	40.498	124.294	a

Table A1 (cont.)

Site Name	Site Number*	Az1	Az2	Dist (km)	Lat. N	Lon. W	Class
<b><u>Landers, June 28, 1992, M=7.3</u></b>							
Twenty-nine Palms	(cdmg 22161)	90	0	41.9	34.021	116.009	a
Silent Valley	(cdmg 12206)	90	0	51.3	33.851	116.852	a
Joshua Tree	(cdmg 22170)	90	0	11.3	34.131	116.314	b
Desert hot Springs	(cdmg 12149)	90	0	22.5	33.962	116.509	b
Barstow	(cdmg 23559)	90	0	37.7	34.887	117.047	b
Fort Irwin	(cdmg 24577)	90	0	65.0	35.268	116.684	b
Yermo	(cdmg 22074)	90	0	26.3	34.903	116.823	c
Palm Springs	(cdmg 12025)	90	0	36.7	33.829	116.501	c
Indio	(cdmg 12026)	90	0	54.9	33.717	116.156	c
Amboy	(cdmg 21081)	90	0	68.3	34.560	115.743	a
Baker	(cdmg 32075)	140	50	88.3	35.272	116.066	b
Boron	(cdmg 33083)	90	0	92.4	35.002	117.650	b
Hemet	(cdmg 12331)	90	0	69.1	33.729	116.979	c
Puerta La Cruz	(cdmg 12168)	90	0	95.0	33.324	116.683	b
Riverside Airport	(cdmg 13123)	270	180	96.2	33.951	117.446	b
San Bernardino E & H	(cdmg 23542)	90	180	79.9	34.065	117.292	c
N. Palm Sprngs fs	(usgs 5295)	180	90	27.7	33.924	116.543	b
Whitewater Canyon	(usgs 5072)	270	180	27.6	33.989	116.655	a
Morongo Valley	(usgs 5071)	135	45	17.7	34.048	116.577	b
Forest Falls	(usgs 5075)	300	210	45.4	34.088	116.919	b
Indio Jackson rd	(usgs 5294)	180	90	49.6	33.747	116.214	c
Fun Valley	(usgs 5069)	135	45	25.8	33.930	116.390	b
Thousand Palms	(usgs 5068)	135	45	37.7	33.820	116.400	c
Euclid st., Fountain Valley	(usc 02)	22	292	144.2	33.719	117.938	c
Roscoe Blvd., Sun Valley	(usc 06)	90	0	162.8	34.221	118.421	b
Buena Vista St., Burbank	(usc 12)	340	250	157.2	34.168	118.332	c
924 W. 70th St., LA	(usc 23)	0	270	163.0	33.976	118.289	c
5921 N. Figueroa St., LA	(usc 32)	58	328	147.8	34.111	118.189	b
3036 Fletcher Dr., LA	(usc 34)	234	144	152.2	34.115	118.244	c
N. Las Virgines Rd., Calabasas	(usc 52)	290	200	189.4	34.151	118.697	b
Mt. Gleason Ave., Sunland	(usc 58)	260	170	150.8	34.269	118.303	b
Big Tujunga Station	(usc 61)	352	262	143.4	34.286	118.225	b
Las Palmas Ave., Glendale	(usc 63)	267	177	147.3	34.200	118.231	c
120 N. Oakbank, Glendora	(usc 65)	170	80	121.5	34.137	117.882	b
Colima Rd., Hacienda Heights	(usc 73)	230	140	135.1	33.990	117.942	c
180 Campus Dr., Arcadia	(usc 93)	9	279	134.3	34.130	118.036	b
<b><u>Big Bear, June 28, 1992, M=6.2</u></b>							
Big Bear Lake - civic center	(cdmg 22561)	270	360	10.2	34.238	116.935	b
San Bernardino E & H	(cdmg 23542)	90	180	39.7	34.065	117.292	c
N. Palm Springs FS	(usgs 5295)	180	90	36.2	33.924	116.543	b
San Bernardino, Highland FS	(usgs 5161)	315	225	31.3	34.136	117.213	c
Morongo Valley	(usgs 5071)	135	45	24.6	34.048	116.577	b
Fun Valley	(usgs 5069)	135	45	45.7	33.930	116.390	b
Euclid st., Fountain Valley	(usc 02)	22	292	109.2	33.719	117.938	c
120 N. Oakbank, Glendora	(usc 65)	170	80	93.0	34.137	117.882	b
656 S. Grand Ave., Covina	(usc 68)	74	344	92.4	34.078	117.871	c
1271 W. Badillo, Covina	(usc 70)	0	270	96.3	34.087	117.915	c
504 Rimgrove Ave., La Puente	(usc 72)	105	15	97.4	34.026	117.918	c
Colima Rd., Hacienda Heights	(usc 73)	230	140	100.2	33.990	117.942	c
E. Joslin St., Santa Fe Springs	(usc 77)	120	30	114.3	33.944	118.087	c

Site Name	Site	Number*	Az1	Az2	Dist (km)	Lat. N	Lon. W	Class
17852 Serrano Ave., Villa Park	(usc 90)	0	270		94.4	33.821	117.818	b
180 Campus Dr., Arcadia	(usc 93)	9	279		107.2	34.130	118.036	b
7420 Jaboneria, Bell Gardens	(usc 94)	310	220		120.3	33.965	118.158	c
<b><i>Northridge, Jan. 17, 1994, M=6.7</i></b>								
Alhambra - Fremont Sch.	(cdmg 24461)	90	360		36.2	34.070	118.150	b
Castaic Old Ridge Rt.	(cdmg 24278)	90	360		20.8	34.564	118.642	b
Century City - LACC north	(cdmg 24389)	90	360		17.4	34.063	118.418	c
Lake Hughes #1 fs	(cdmg 24271)	90	0		36.1	34.674	118.430	b
Lake Hughes 4	(cdmg 24469)	90	0		31.9	34.650	118.478	c
Lake Hughes #4b	(cdmg 24523)	90	0		32.0	34.650	118.477	c
Lake Hughes #9	(cdmg 24272)	90	360		25.6	34.608	118.558	a
Lake Hughes #12a	(cdmg 24607)	90	180		21.5	34.571	118.560	b
Littlerock - Brainard Canyon	(cdmg 23595)	90	180		46.7	34.486	117.980	a
Long Beach - City Hall grds.	(cdmg 14560)	90	360		56.0	33.768	118.196	c
LA - Hollywood stor.blg.	(cdmg 24303)	90	360		20.0	34.090	118.339	c
Mt. Baldy - Elem. School	(cdmg 23572)	90	180		72.2	34.233	117.661	a
Mt. Wilson	(cdmg 24399)	90	360		36.5	34.224	118.057	a
Phelan - Wilson Ranch Rd.	(cdmg 23597)	90	180		86.4	34.467	117.520	b
Port Hueneme - Naval Lab.	(cdmg 25281)	180	90		49.8	34.145	119.206	c
Rancho Cucamnga-Deer Can.	(cdmg 23598)	90	180		80.8	34.169	117.579	a
Rancho Cucamnga - L&J FF	(cdmg 23497)	90	0		82.9	34.104	117.574	b
Rancho Palos Verdes	(cdmg 14404)	90	0		50.8	33.746	118.396	a
Riverside airport	(cdmg 13123)	270	180		99.8	33.951	117.446	b
San Bernardino - E & H	(cdmg 23542)	90	180		109.2	34.065	117.292	c
Sylmar - Co. Hospital PL	(cdmg 24514)	90	360		1.7	34.326	118.444	c
Tarzana Cedar Hill Nur. A	(cdmg 24436)	90	360		3.4	34.160	118.534	b
Wrightwood - Jackson Flat	(cdmg 23590)	90	180		65.2	34.381	117.737	a
Wrightwood-Nielson Rnch	(cdmg 23573)	90	180		82.4	34.314	117.545	b
Wrightwood-Swarthout Vly.	(cdmg 23574)	90	180		72.3	34.369	117.658	b
17645 Saticoy St. Northridge	(usc 03)	180	90		0.2	34.209	118.517	c
12001 Chalon Rd. LA	(usc 15)	70	160		12.4	34.086	118.481	b
700 N. Faring Rd, LA	(usc 16)	0	90		14.1	34.089	118.435	b
8510 Wonderland Ave, LA	(usc 17)	185	95		15.4	34.114	118.380	a
Willoughby Ave. Hollywood	(usc 18)	180	90		18.3	34.088	118.365	b
600 E. Grand Av., San Gabriel	(usc 19)	180	270		39.4	34.091	118.093	b
2628 W. 15th. St., LA	(usc 20)	180	90		26.1	34.045	118.298	c
4312 S. Grand Ave, LA	(usc 22)	180	90		30.4	34.005	118.279	c
2369 E. Vernon Ave, LA	(usc 25)	180	90		33.8	34.004	118.230	c
624 Cypress Ave., LA	(usc 33)	53	143		29.4	34.088	118.222	b
3036 Fletcher Dr., LA	(usc 34)	144	234		26.2	34.115	118.244	c
23536 Catskill Ave., Carson	(usc 40)	180	90		48.3	33.812	118.270	c
Rancho Palos Verdes	(usc 44)	5	95		53.1	33.740	118.335	c
14801 Osage Ave, Lawndale	(usc 45)	182	92		36.7	33.897	118.346	c
Manhattan Beach	(usc 46)	0	90		36.1	33.886	118.389	c
Canoga Park	(usc 53)	196	106		1.6	34.212	118.606	c
3960 Centinela St., LA	(usc 54)	155	245		22.9	34.001	118.431	c
Canyon Country	(usc 57)	0	270		11.4	34.419	118.426	c
1250 Howard rd., Burbank	(usc 59)	330	60		16.5	34.204	118.302	a
New York Ave., La Crescenta	(usc 60)	180	90		18.8	34.238	118.254	c
Big Tujunga Station	(usc 61)	352	262		19.9	34.286	118.225	b
3320 Las Palmas Ave., Glendale	(usc 63)	177	267		22.3	34.200	118.231	b

Site Name	Site Number*	Az1	Az2	Dist (km)	Lat. N	Lon. W	Class
Fairview Ave., El Monte	(usc 66)	185	95	45.2	34.093	118.019	c
237 Mel Canyon Rd., Duarte	(usc 67)	90	180	49.3	34.150	117.939	b
656 S. Grand Ave., Covina	(usc 68)	344	74	58.1	34.078	117.871	c
3699 Holly Ave., Baldwin Park	(usc 69)	180	270	48.5	34.100	117.974	b
1271 W. Badillo, Covina	(usc 70)	360	270	54.0	34.087	117.915	c
S. Orange Ave., West Covina	(usc 71)	315	225	52.1	34.064	117.952	c
504 Rimgrove Ave., La Puente	(usc 72)	15	105	57.0	34.026	117.918	c
Colima Rd., Hacienda Heights	(usc 73)	140	230	57.3	33.990	117.942	c
6302 S. Alta Dr. Whittier	(usc 75)	0	90	48.9	34.015	118.029	b
E. Joslin St., Santa Fe Springs	(usc 77)	30	120	48.3	33.944	118.087	c
14637 Castlegate st., Compton	(usc 78)	360	270	44.2	33.899	118.196	c
21288 Water St., Carson	(usc 81)	180	270	47.4	33.836	118.240	c
Terminal Island	(usc 82)	330	240	55.8	33.736	118.269	c
Huntington Beach	(usc 83)	290	200	67.9	33.727	118.044	c
Del Amo Blvd., Lakewood	(usc 84)	0	90	54.6	33.846	118.099	c
6861 Santa Rita, Garden Grove	(usc 85)	360	270	64.7	33.790	118.012	c
La Palma ave., Buena Park	(usc 86)	180	90	60.0	33.847	118.018	c
200 S. Flower Ave., Brea	(usc 87)	20	290	64.9	33.916	117.896	c
2000 W. Ball Rd., Anaheim	(usc 88)	0	90	66.9	33.817	117.951	c
5360 Saturn St., LA	(usc 91)	20	110	22.3	34.046	118.355	c
180 Campus Dr., Arcadia	(usc 93)	9	279	41.9	34.130	118.036	b
7420 Jaboneria, Bell Gardens	(usc 94)	310	220	41.7	33.965	118.158	c
3620 S. Vermont Ave., LA	(usc 96)	0	90	28.1	34.022	118.293	c
855 Arcadia Ave., Arcadia	(usc 99)	172	262	40.1	34.127	118.059	c
Griffith Observatory	(usgs 141)	360	270	21.5	34.118	118.299	a
Littlerock Post Office	(usgs 5030)	300	210	47.6	34.520	117.990	b
Pardo Dam Downstream	(usgs 969)	90	360	86.7	33.890	117.641	c
Long Beach VA Hospital	(usgs 5106)	360	270	59.2	33.778	118.118	b
NSMP Pasadena Lab.	(usgs 5296)	360	270	34.1	34.136	118.127	b

\* ct: California Institute of Technology Civil Engineering Dept.  
 usc: University of Southern California Civil Engineering Dept.  
 cdmg: California Division of Mines and Geology Strong Motion Instrumentation Program  
 usgs: U. S. Geological Survey National Strong Motion Program

Table A2. Regression coefficients for peak ground acceleration *PGA* and velocity, *PGV*

PGA							
<i>a</i>	<i>b</i>	<i>c</i>	<i>d</i>	<i>h</i>	<i>e</i>	<i>f</i>	$\sigma$
3.098	0.3065	-0.07570	-0.8795	6.910	0.1452	0.1893	0.2124
PGV							
<i>a</i>	<i>b</i>	<i>c</i>	<i>d</i>	<i>h</i>	<i>e</i>	<i>f</i>	$\sigma$
1.747	0.4481	-0.03248	-0.8075	3.992	0.1862	0.3009	0.2470

Regression coefficients refer to a randomly oriented horizontal component, for the base 10

logarithm of motion,  $PGA$  in units of  $\text{cm/sec}^2$  and  $PGV$  in units of  $\text{cm/sec}$ .  
 Table A3. Regression coefficients for  $PSV$ , 2% damping, base 10 logarithm of motion, randomly oriented horizontal component ( $\text{cm/sec}$ ).

<i>Freq. (Hz)</i>	<i>a</i>	<i>b</i>	<i>c</i>	<i>d</i>	<i>h</i>	<i>e</i>	<i>f</i>	$\sigma$
0.500	1.581	0.638	-0.037	-0.695	2.773	0.267	0.452	0.326
0.526	1.588	0.631	-0.061	-0.693	3.123	0.293	0.474	0.327
0.556	1.614	0.627	-0.070	-0.694	3.427	0.296	0.471	0.326
0.588	1.637	0.607	-0.060	-0.693	3.512	0.290	0.468	0.319
0.625	1.700	0.599	-0.059	-0.731	3.664	0.291	0.472	0.311
0.667	1.715	0.586	-0.033	-0.748	3.476	0.303	0.476	0.302
0.714	1.709	0.569	-0.039	-0.717	2.966	0.282	0.450	0.302
0.769	1.745	0.541	-0.047	-0.708	2.945	0.260	0.429	0.306
0.833	1.814	0.544	-0.070	-0.703	3.340	0.216	0.388	0.290
0.909	1.774	0.524	-0.079	-0.658	3.163	0.213	0.391	0.288
1.000	1.844	0.501	-0.045	-0.700	3.723	0.219	0.372	0.277
1.053	1.871	0.496	-0.039	-0.724	3.383	0.223	0.368	0.282
1.111	1.891	0.500	-0.043	-0.738	3.201	0.218	0.368	0.287
1.176	1.875	0.497	-0.047	-0.733	2.881	0.226	0.376	0.284
1.250	1.866	0.493	-0.060	-0.716	2.674	0.202	0.361	0.290
1.333	1.915	0.494	-0.074	-0.753	2.850	0.224	0.368	0.292
1.429	1.974	0.505	-0.082	-0.796	3.304	0.221	0.375	0.294
1.538	2.013	0.463	-0.057	-0.798	3.472	0.183	0.343	0.291
1.667	2.023	0.465	-0.087	-0.795	3.717	0.197	0.335	0.292
1.818	1.973	0.406	-0.065	-0.741	3.512	0.195	0.340	0.279
2.000	2.001	0.390	-0.057	-0.768	4.388	0.224	0.352	0.269
2.083	1.985	0.380	-0.053	-0.757	4.137	0.219	0.343	0.271
2.174	1.958	0.364	-0.051	-0.733	3.963	0.213	0.337	0.274
2.273	1.986	0.368	-0.053	-0.742	3.952	0.188	0.307	0.278
2.381	2.023	0.367	-0.069	-0.761	4.186	0.187	0.287	0.274
2.500	2.045	0.333	-0.043	-0.777	4.538	0.177	0.283	0.268
2.632	2.099	0.321	-0.043	-0.804	5.036	0.158	0.256	0.262
2.778	2.096	0.338	-0.063	-0.814	5.274	0.182	0.266	0.266
2.941	2.122	0.341	-0.080	-0.814	5.361	0.165	0.235	0.262
3.125	2.101	0.349	-0.090	-0.809	5.413	0.166	0.235	0.262
3.333	2.083	0.358	-0.116	-0.796	5.859	0.171	0.237	0.255
3.571	2.204	0.370	-0.131	-0.867	7.914	0.153	0.198	0.246
3.846	2.160	0.359	-0.123	-0.858	8.085	0.154	0.186	0.243
4.167	2.219	0.362	-0.121	-0.906	8.782	0.143	0.170	0.243
4.545	2.193	0.350	-0.129	-0.895	9.549	0.151	0.165	0.238
5.000	2.325	0.370	-0.163	-0.962	11.380	0.117	0.116	0.238
5.263	2.271	0.363	-0.166	-0.953	10.400	0.125	0.130	0.238
5.556	2.275	0.335	-0.155	-0.975	10.590	0.132	0.130	0.241
5.882	2.200	0.318	-0.156	-0.953	10.870	0.155	0.145	0.243
6.250	2.313	0.303	-0.140	-1.029	12.470	0.130	0.126	0.241
6.667	2.314	0.310	-0.150	-1.052	12.850	0.123	0.121	0.239
7.143	2.325	0.301	-0.134	-1.111	12.850	0.147	0.139	0.243
7.692	2.265	0.299	-0.124	-1.098	12.920	0.124	0.117	0.240
8.333	2.185	0.308	-0.128	-1.085	11.860	0.098	0.101	0.234
9.091	2.096	0.252	-0.079	-1.092	11.400	0.112	0.113	0.252
10.00	2.061	0.254	-0.090	-1.096	11.570	0.091	0.087	0.247

Table A4. Regression coefficients for *PSV*, 5% damping, base 10 logarithm of motion, randomly oriented horizontal component (cm/sec).

<i>Freq. (Hz)</i>	<i>a</i>	<i>b</i>	<i>c</i>	<i>d</i>	<i>h</i>	<i>e</i>	<i>f</i>	$\sigma$
0.500	1.547	0.627	-0.046	-0.729	2.929	0.275	0.449	0.316
0.526	1.563	0.621	-0.066	-0.724	3.145	0.279	0.451	0.318
0.556	1.572	0.609	-0.065	-0.722	3.302	0.287	0.456	0.315
0.588	1.593	0.597	-0.065	-0.722	3.400	0.288	0.459	0.310
0.625	1.634	0.588	-0.063	-0.744	3.543	0.294	0.464	0.304
0.667	1.648	0.575	-0.048	-0.755	3.390	0.300	0.463	0.299
0.714	1.654	0.554	-0.046	-0.733	3.005	0.276	0.433	0.297
0.769	1.713	0.542	-0.055	-0.739	3.121	0.243	0.404	0.297
0.833	1.767	0.530	-0.061	-0.739	3.401	0.211	0.380	0.285
0.909	1.750	0.516	-0.074	-0.706	3.302	0.204	0.374	0.283
1.000	1.789	0.490	-0.047	-0.730	3.561	0.216	0.368	0.277
1.053	1.822	0.489	-0.043	-0.753	3.420	0.213	0.360	0.279
1.111	1.834	0.487	-0.043	-0.765	3.182	0.211	0.361	0.283
1.176	1.830	0.486	-0.045	-0.771	2.983	0.222	0.371	0.284
1.250	1.830	0.481	-0.054	-0.768	2.914	0.217	0.368	0.285
1.333	1.869	0.480	-0.062	-0.796	3.087	0.225	0.370	0.287
1.429	1.904	0.482	-0.072	-0.812	3.367	0.214	0.363	0.292
1.538	1.939	0.454	-0.052	-0.823	3.503	0.189	0.344	0.288
1.667	1.930	0.442	-0.072	-0.810	3.562	0.200	0.341	0.286
1.818	1.923	0.406	-0.061	-0.792	3.850	0.204	0.342	0.277
2.000	1.914	0.376	-0.049	-0.787	4.116	0.217	0.350	0.270
2.083	1.898	0.362	-0.046	-0.774	3.955	0.214	0.344	0.271
2.174	1.885	0.350	-0.042	-0.759	3.942	0.204	0.332	0.271
2.273	1.894	0.344	-0.041	-0.761	3.999	0.191	0.315	0.272
2.381	1.929	0.344	-0.051	-0.779	4.208	0.181	0.296	0.270
2.500	1.964	0.329	-0.048	-0.799	4.545	0.173	0.283	0.264
2.632	1.972	0.315	-0.048	-0.807	4.767	0.171	0.278	0.262
2.778	1.981	0.324	-0.059	-0.818	4.948	0.179	0.274	0.264
2.941	1.998	0.322	-0.066	-0.826	5.236	0.178	0.262	0.260
3.125	1.997	0.335	-0.085	-0.824	5.409	0.177	0.249	0.256
3.333	1.998	0.340	-0.105	-0.824	5.854	0.177	0.240	0.248
3.571	2.060	0.344	-0.111	-0.865	7.022	0.164	0.211	0.242
3.846	2.082	0.346	-0.114	-0.885	7.589	0.156	0.187	0.237
4.167	2.090	0.347	-0.115	-0.906	8.303	0.157	0.188	0.236
4.545	2.101	0.341	-0.127	-0.915	9.229	0.152	0.175	0.232
5.000	2.181	0.350	-0.149	-0.962	10.670	0.132	0.138	0.230
5.263	2.153	0.345	-0.151	-0.964	10.270	0.139	0.144	0.229
5.556	2.146	0.334	-0.150	-0.976	10.260	0.139	0.143	0.230
5.882	2.102	0.319	-0.151	-0.967	10.450	0.148	0.149	0.232
6.250	2.115	0.301	-0.133	-0.990	10.790	0.136	0.137	0.229
6.667	2.108	0.300	-0.133	-1.010	11.050	0.130	0.130	0.230
7.143	2.121	0.297	-0.126	-1.053	11.670	0.141	0.146	0.228
7.692	2.057	0.285	-0.109	-1.047	11.570	0.138	0.144	0.225
8.333	1.986	0.284	-0.106	-1.033	10.850	0.114	0.123	0.224
9.091	1.915	0.254	-0.075	-1.044	10.540	0.120	0.135	0.233
10.000	1.857	0.248	-0.071	-1.044	10.430	0.112	0.121	0.230

Table A5. Regression coefficients for PSV, 10% damping, base 10 logarithm of motion, randomly oriented horizontal component (cm/sec).

Freq. (Hz)	a	b	c	d	h	e	f	$\sigma$
0.500	1.488	0.612	-0.053	-0.739	3.006	0.271	0.439	0.309
0.526	1.509	0.605	-0.062	-0.742	3.142	0.276	0.440	0.308
0.556	1.526	0.601	-0.067	-0.743	3.227	0.277	0.439	0.307
0.588	1.546	0.590	-0.067	-0.746	3.324	0.280	0.441	0.303
0.625	1.569	0.581	-0.065	-0.756	3.389	0.284	0.447	0.300
0.667	1.581	0.564	-0.056	-0.757	3.346	0.285	0.444	0.297
0.714	1.602	0.544	-0.051	-0.754	3.173	0.269	0.425	0.295
0.769	1.653	0.534	-0.053	-0.757	3.233	0.237	0.396	0.291
0.833	1.698	0.524	-0.058	-0.759	3.391	0.211	0.375	0.285
0.909	1.703	0.506	-0.054	-0.747	3.370	0.201	0.368	0.283
1.000	1.719	0.484	-0.042	-0.753	3.433	0.209	0.365	0.279
1.053	1.739	0.479	-0.041	-0.765	3.381	0.208	0.361	0.280
1.111	1.759	0.473	-0.039	-0.781	3.259	0.212	0.363	0.281
1.176	1.768	0.471	-0.043	-0.791	3.134	0.215	0.366	0.281
1.250	1.773	0.472	-0.054	-0.797	3.134	0.221	0.370	0.282
1.333	1.797	0.470	-0.059	-0.811	3.261	0.221	0.366	0.284
1.429	1.822	0.463	-0.059	-0.819	3.384	0.209	0.355	0.287
1.538	1.838	0.438	-0.045	-0.824	3.469	0.198	0.347	0.284
1.667	1.840	0.422	-0.051	-0.819	3.573	0.197	0.341	0.284
1.818	1.838	0.400	-0.056	-0.806	3.870	0.203	0.341	0.276
2.000	1.827	0.365	-0.044	-0.793	3.919	0.204	0.336	0.270
2.083	1.818	0.352	-0.041	-0.787	3.891	0.202	0.333	0.270
2.174	1.820	0.345	-0.040	-0.786	3.933	0.195	0.324	0.268
2.273	1.828	0.340	-0.041	-0.789	4.013	0.188	0.315	0.267
2.381	1.847	0.333	-0.042	-0.799	4.198	0.182	0.304	0.266
2.500	1.861	0.325	-0.043	-0.808	4.433	0.178	0.296	0.262
2.632	1.862	0.315	-0.043	-0.814	4.547	0.178	0.292	0.262
2.778	1.865	0.308	-0.045	-0.821	4.716	0.183	0.289	0.261
2.941	1.882	0.312	-0.060	-0.828	5.076	0.181	0.275	0.256
3.125	1.894	0.321	-0.075	-0.833	5.419	0.182	0.258	0.252
3.333	1.910	0.326	-0.088	-0.845	5.814	0.179	0.243	0.245
3.571	1.945	0.332	-0.094	-0.870	6.477	0.166	0.218	0.240
3.846	1.954	0.338	-0.105	-0.882	6.968	0.160	0.202	0.236
4.167	1.960	0.337	-0.110	-0.896	7.619	0.161	0.198	0.232
4.545	1.980	0.336	-0.122	-0.909	8.460	0.147	0.177	0.226
5.000	1.999	0.335	-0.133	-0.931	9.285	0.141	0.158	0.223
5.263	1.997	0.338	-0.140	-0.941	9.477	0.145	0.157	0.221
5.556	1.991	0.334	-0.143	-0.950	9.512	0.142	0.154	0.221
5.882	1.964	0.324	-0.141	-0.950	9.492	0.141	0.152	0.222
6.250	1.954	0.308	-0.129	-0.961	9.630	0.135	0.146	0.222
6.667	1.934	0.301	-0.123	-0.972	9.669	0.132	0.143	0.222
7.143	1.916	0.296	-0.117	-0.988	10.060	0.137	0.151	0.220
7.692	1.860	0.290	-0.108	-0.984	9.992	0.138	0.155	0.218
8.333	1.818	0.286	-0.102	-0.985	9.791	0.125	0.143	0.217
9.091	1.760	0.272	-0.086	-0.994	9.648	0.130	0.151	0.219
10.000	1.692	0.258	-0.071	-0.990	9.442	0.126	0.146	0.215

Table A6. Regression coefficients for  $V_{ea}$ , 2% damping, base 10 logarithm of motion, randomly oriented horizontal component (cm/sec).

Freq. (Hz)	a	b	c	d	h	e	f	$\sigma$
0.500	1.691	0.655	-0.046	-0.653	2.791	0.236	0.426	0.318
0.526	1.689	0.649	-0.066	-0.661	3.176	0.282	0.465	0.320
0.556	1.705	0.629	-0.060	-0.658	3.593	0.288	0.476	0.316
0.588	1.748	0.626	-0.071	-0.656	3.783	0.273	0.460	0.312
0.625	1.811	0.625	-0.064	-0.698	3.892	0.276	0.468	0.300
0.667	1.821	0.603	-0.027	-0.719	3.691	0.296	0.477	0.291
0.714	1.840	0.592	-0.032	-0.711	3.446	0.283	0.462	0.292
0.769	1.821	0.562	-0.044	-0.662	2.862	0.264	0.438	0.292
0.833	1.869	0.569	-0.079	-0.647	2.978	0.233	0.413	0.282
0.909	1.855	0.538	-0.069	-0.614	3.108	0.225	0.405	0.277
1.000	1.931	0.524	-0.043	-0.657	3.674	0.219	0.386	0.262
1.053	1.962	0.517	-0.040	-0.675	3.275	0.211	0.371	0.267
1.111	1.990	0.526	-0.051	-0.693	3.217	0.219	0.379	0.270
1.176	1.970	0.510	-0.044	-0.678	2.778	0.219	0.380	0.267
1.250	1.948	0.525	-0.072	-0.658	2.573	0.210	0.368	0.266
1.333	2.001	0.525	-0.069	-0.696	2.594	0.218	0.371	0.267
1.429	2.043	0.529	-0.080	-0.726	3.030	0.220	0.385	0.270
1.538	2.099	0.494	-0.059	-0.743	3.369	0.195	0.364	0.269
1.667	2.103	0.503	-0.089	-0.735	3.419	0.203	0.353	0.270
1.818	2.083	0.431	-0.050	-0.685	3.269	0.192	0.342	0.258
2.000	2.125	0.426	-0.047	-0.722	4.246	0.211	0.344	0.251
2.083	2.105	0.431	-0.055	-0.716	4.261	0.220	0.351	0.252
2.174	2.090	0.418	-0.053	-0.697	3.881	0.213	0.342	0.252
2.273	2.113	0.418	-0.064	-0.692	3.735	0.187	0.315	0.248
2.381	2.132	0.421	-0.074	-0.704	3.854	0.190	0.295	0.249
2.500	2.156	0.390	-0.042	-0.720	4.186	0.177	0.286	0.247
2.632	2.218	0.384	-0.041	-0.749	4.515	0.150	0.256	0.240
2.778	2.209	0.392	-0.066	-0.740	4.537	0.163	0.254	0.238
2.941	2.244	0.402	-0.074	-0.758	4.877	0.155	0.234	0.242
3.125	2.195	0.401	-0.084	-0.730	4.561	0.164	0.246	0.237
3.333	2.194	0.424	-0.102	-0.736	4.902	0.160	0.251	0.229
3.571	2.269	0.421	-0.102	-0.775	6.383	0.147	0.213	0.218
3.846	2.221	0.427	-0.107	-0.765	6.442	0.158	0.214	0.220
4.167	2.286	0.421	-0.086	-0.811	6.651	0.137	0.192	0.215
4.545	2.216	0.433	-0.099	-0.774	6.334	0.151	0.185	0.210
5.000	2.312	0.445	-0.118	-0.816	7.549	0.111	0.141	0.209
5.263	2.301	0.445	-0.128	-0.815	6.902	0.105	0.140	0.207
5.556	2.268	0.427	-0.113	-0.826	6.910	0.136	0.170	0.210
5.882	2.223	0.424	-0.114	-0.819	6.870	0.158	0.186	0.206
6.250	2.251	0.411	-0.098	-0.839	7.204	0.139	0.167	0.201
6.667	2.268	0.411	-0.097	-0.860	7.594	0.132	0.159	0.199
7.143	2.234	0.423	-0.102	-0.864	7.228	0.138	0.170	0.196
7.692	2.215	0.411	-0.068	-0.884	7.198	0.131	0.173	0.200
8.333	2.148	0.410	-0.061	-0.860	6.398	0.123	0.174	0.197
9.091	2.108	0.402	-0.040	-0.871	6.230	0.133	0.191	0.205
10.000	2.042	0.402	-0.042	-0.849	5.715	0.130	0.194	0.212

Table A7. Regression coefficients for  $V_{ea}$ , 5% damping, base 10 logarithm of motion, randomly oriented horizontal component (cm/sec).

<i>Freq. (Hz)</i>	<i>a</i>	<i>b</i>	<i>c</i>	<i>d</i>	<i>h</i>	<i>e</i>	<i>f</i>	$\sigma$
0.500	1.686	0.637	-0.050	-0.646	2.873	0.250	0.435	0.293
0.526	1.698	0.630	-0.059	-0.651	3.175	0.272	0.454	0.294
0.556	1.715	0.618	-0.062	-0.651	3.474	0.279	0.464	0.290
0.588	1.747	0.613	-0.068	-0.655	3.622	0.277	0.462	0.287
0.625	1.785	0.606	-0.057	-0.677	3.653	0.278	0.464	0.280
0.667	1.808	0.591	-0.039	-0.696	3.570	0.289	0.469	0.273
0.714	1.824	0.577	-0.041	-0.687	3.307	0.278	0.453	0.272
0.769	1.824	0.561	-0.055	-0.653	2.921	0.260	0.432	0.269
0.833	1.855	0.554	-0.073	-0.642	2.961	0.242	0.416	0.262
0.909	1.862	0.528	-0.061	-0.627	3.161	0.234	0.407	0.255
1.000	1.915	0.520	-0.050	-0.648	3.330	0.218	0.381	0.247
1.053	1.947	0.519	-0.050	-0.667	3.240	0.213	0.372	0.249
1.111	1.971	0.517	-0.050	-0.682	3.163	0.215	0.373	0.250
1.176	1.962	0.513	-0.053	-0.675	2.897	0.217	0.374	0.248
1.250	1.960	0.516	-0.064	-0.669	2.704	0.212	0.369	0.247
1.333	1.996	0.514	-0.065	-0.694	2.764	0.212	0.368	0.249
1.429	2.029	0.506	-0.066	-0.713	3.055	0.211	0.372	0.253
1.538	2.069	0.490	-0.065	-0.726	3.324	0.200	0.361	0.252
1.667	2.077	0.483	-0.078	-0.718	3.439	0.202	0.350	0.249
1.818	2.074	0.439	-0.054	-0.694	3.502	0.199	0.339	0.241
2.000	2.091	0.427	-0.050	-0.707	4.134	0.211	0.340	0.236
2.083	2.081	0.426	-0.055	-0.700	4.119	0.212	0.339	0.236
2.174	2.080	0.421	-0.058	-0.692	3.985	0.204	0.328	0.235
2.273	2.093	0.416	-0.063	-0.690	3.937	0.192	0.310	0.233
2.381	2.107	0.412	-0.065	-0.696	3.988	0.187	0.295	0.232
2.500	2.131	0.399	-0.056	-0.710	4.215	0.178	0.283	0.230
2.632	2.160	0.393	-0.056	-0.721	4.398	0.162	0.263	0.227
2.778	2.175	0.397	-0.068	-0.728	4.561	0.162	0.252	0.225
2.941	2.194	0.400	-0.077	-0.737	4.868	0.159	0.241	0.224
3.125	2.180	0.405	-0.087	-0.729	4.868	0.162	0.242	0.221
3.333	2.182	0.420	-0.099	-0.735	5.170	0.161	0.241	0.215
3.571	2.213	0.425	-0.106	-0.754	6.042	0.154	0.219	0.207
3.846	2.204	0.426	-0.105	-0.761	6.330	0.157	0.212	0.205
4.167	2.233	0.425	-0.095	-0.787	6.468	0.144	0.195	0.203
4.545	2.210	0.433	-0.102	-0.777	6.522	0.145	0.181	0.199
5.000	2.262	0.442	-0.117	-0.803	7.261	0.122	0.153	0.199
5.263	2.257	0.440	-0.121	-0.807	7.026	0.120	0.152	0.198
5.556	2.240	0.431	-0.115	-0.815	7.070	0.134	0.166	0.198
5.882	2.222	0.424	-0.109	-0.823	7.155	0.148	0.178	0.196
6.250	2.225	0.417	-0.099	-0.836	7.297	0.142	0.172	0.193
6.667	2.228	0.417	-0.097	-0.848	7.368	0.134	0.164	0.191
7.143	2.203	0.419	-0.091	-0.855	7.212	0.134	0.169	0.190
7.692	2.176	0.416	-0.072	-0.866	6.935	0.130	0.174	0.193
8.333	2.123	0.413	-0.060	-0.855	6.425	0.125	0.178	0.194
9.091	2.079	0.412	-0.049	-0.857	6.184	0.132	0.190	0.200
10.000	2.027	0.413	-0.047	-0.846	5.804	0.132	0.197	0.207

Table A8. Regression coefficients for Vea, 10% damping, base 10 logarithm of motion, randomly oriented horizontal component (cm/sec).

<i>Freq. (Hz)</i>	<i>a</i>	<i>b</i>	<i>c</i>	<i>d</i>	<i>h</i>	<i>e</i>	<i>f</i>	$\sigma$
0.500	1.712	0.610	-0.048	-0.643	3.040	0.256	0.436	0.269
0.526	1.727	0.605	-0.053	-0.646	3.219	0.265	0.445	0.268
0.556	1.742	0.598	-0.057	-0.648	3.384	0.272	0.451	0.266
0.588	1.764	0.592	-0.058	-0.653	3.468	0.275	0.453	0.264
0.625	1.790	0.584	-0.053	-0.663	3.481	0.275	0.453	0.260
0.667	1.813	0.574	-0.047	-0.672	3.419	0.275	0.450	0.256
0.714	1.831	0.562	-0.048	-0.666	3.263	0.267	0.438	0.254
0.769	1.843	0.549	-0.057	-0.651	3.055	0.255	0.424	0.250
0.833	1.862	0.538	-0.064	-0.640	3.052	0.243	0.411	0.245
0.909	1.883	0.521	-0.057	-0.637	3.189	0.234	0.399	0.240
1.000	1.921	0.512	-0.052	-0.650	3.272	0.222	0.380	0.235
1.053	1.944	0.510	-0.052	-0.661	3.239	0.217	0.372	0.235
1.111	1.962	0.507	-0.052	-0.670	3.160	0.215	0.369	0.235
1.176	1.970	0.504	-0.055	-0.673	3.049	0.214	0.366	0.234
1.250	1.981	0.502	-0.058	-0.678	2.972	0.212	0.363	0.234
1.333	2.003	0.498	-0.060	-0.691	3.015	0.210	0.362	0.235
1.429	2.031	0.490	-0.062	-0.704	3.192	0.208	0.360	0.238
1.538	2.058	0.479	-0.064	-0.712	3.408	0.203	0.353	0.237
1.667	2.070	0.465	-0.067	-0.709	3.555	0.202	0.344	0.235
1.818	2.076	0.440	-0.057	-0.701	3.761	0.203	0.336	0.229
2.000	2.083	0.427	-0.055	-0.702	4.109	0.205	0.330	0.226
2.083	2.084	0.423	-0.057	-0.699	4.154	0.203	0.325	0.224
2.174	2.085	0.419	-0.060	-0.695	4.132	0.199	0.316	0.223
2.273	2.090	0.415	-0.063	-0.693	4.112	0.193	0.305	0.222
2.381	2.100	0.409	-0.064	-0.696	4.159	0.187	0.293	0.220
2.500	2.116	0.403	-0.063	-0.702	4.286	0.179	0.280	0.218
2.632	2.134	0.399	-0.065	-0.710	4.430	0.169	0.266	0.216
2.778	2.151	0.401	-0.071	-0.718	4.618	0.165	0.254	0.215
2.941	2.163	0.404	-0.079	-0.725	4.855	0.162	0.245	0.213
3.125	2.168	0.409	-0.087	-0.729	5.079	0.162	0.239	0.210
3.333	2.172	0.418	-0.097	-0.734	5.357	0.161	0.233	0.206
3.571	2.185	0.422	-0.102	-0.745	5.848	0.156	0.220	0.200
3.846	2.193	0.424	-0.102	-0.757	6.185	0.152	0.208	0.197
4.167	2.201	0.427	-0.101	-0.770	6.384	0.145	0.195	0.195
4.545	2.206	0.431	-0.105	-0.778	6.624	0.140	0.181	0.192
5.000	2.227	0.436	-0.112	-0.796	7.049	0.130	0.164	0.191
5.263	2.228	0.435	-0.114	-0.804	7.092	0.129	0.164	0.191
5.556	2.220	0.431	-0.111	-0.812	7.117	0.135	0.168	0.190
5.882	2.209	0.426	-0.106	-0.820	7.172	0.141	0.174	0.189
6.250	2.200	0.422	-0.100	-0.827	7.175	0.140	0.173	0.188
6.667	2.189	0.421	-0.095	-0.835	7.140	0.137	0.172	0.187
7.143	2.170	0.419	-0.087	-0.843	7.004	0.135	0.174	0.187
7.692	2.142	0.419	-0.075	-0.849	6.745	0.132	0.178	0.189
8.333	2.103	0.417	-0.064	-0.847	6.399	0.129	0.183	0.192
9.091	2.059	0.416	-0.054	-0.845	6.064	0.131	0.191	0.197
10.000	2.013	0.419	-0.050	-0.839	5.746	0.132	0.199	0.204

## REFERENCES CITED

- Bazzurro, P., and Cornell, C. A., 1998a, Spatial Disaggregation of Seismic Hazard, in *Proceedings, 6th U. S. National Conference on Earthquake Engineering, Seattle, Washington, May 31-June 4, 1998.*
- Bazzurro, P and Cornell, C. A., 1998b,. On Disaggregation of Seismic Hazard, submitted, *Bulletin of the Seismological Society of America*
- Boore, D. M., Joyner, W. B. and Fumal, T. E., 1993, Estimation of response spectra and peak accelerations from western North American earthquakes: An interim report, *U.S. Geol. Survey Open-File Report, 93-509*, 72 pp.
- Boore, D. M., Joyner, W. B. and Fumal, T. E., 1994, Estimation of response spectra and peak accelerations from western North American earthquakes: An interim report, Part 2, *U.S. Geol. Survey Open-File Report, 94-127*, 40 pp.
- Boore, D. M., Joyner, W. B. and Fumal, T. E., 1997, Equations for estimating horizontal response spectra and peak acceleration from western North American earthquakes: a summary of recent work, *Seismological Research Letters*, **68**, 128-153.
- Building Seismic Safety Council (BSSC), 1994, NEHRP recommended provisions for seismic regulations for new buildings, Part 1 - Provisions, *FEMA 222A*, Federal Emergency Management Agency, 290 pp.
- Campbell, K. W., 1997, Empirical near-source attenuation relationships for horizontal and vertical components of peak ground acceleration, peak ground velocity, and pseudo-absolute acceleration response spectra, *Seismological Research Letters*, **68**, 154-179.
- Chapman, M. C., 1995, A probabilistic approach to ground-motion selection for engineering design, *Bulletin of the Seismological Society of America*, **85**, 937-942.
- Cockerham, R. S. and Eaton, J. P., 1987, The earthquake and its aftershocks, April 24 through September 30, 1984, in *The Morgan Hill, California Earthquake of April 24, 1984*, U. S., *Geological Survey Bulletin 1639*, 15-28.
- Cramer, C. H. and Petersen, M. D., 1996, Predominant seismic source distance and magnitude maps for Los Angeles, Orange and Ventura Counties, California, *Bulletin of the Seismological Society of America*, **86**, 1645-1649.
- Harmsen, S. C., Perkins, D. M. and Frankel, A., 1998, Deaggregation of probabilistic ground motions in the central and eastern U.S., submitted to *Bulletin of the Seismological Society of America*.
- Harmsen, S. C. 1997, Determination of site amplification in the Los Angeles urban area from inversion of strong-motion records, *Bulletin of the Seismological Society of America*, **87**, 866-887.
- Hauksson, E., 1994, The 1991 Sierra Madre earthquake sequence in southern California: seismological and tectonic analysis, *Bulletin of the Seismological Society of America*, **84**, 1058-1074.
- Joyner, W. B. and Boore, D. M., 1993, Methods for regression analysis of strong-motion data, *Bulletin of the Seismological Society of America*, **83**, 469-487.
- Joyner, W. B. and Boore, D. M., 1994, Errata, *Bulletin of the Seismological Society of America*, **84**, 955-956.
- Lawson, R. S., 1996, *Site Dependent Inelastic Seismic Demands*, Ph.D. dissertation, Department of Civil Engineering, Stanford University, Stanford, CA, 224 p.
- McGuire, R. K., 1995, Probabilistic seismic hazard analysis and design earthquakes: Closing the loop, *Bulletin of the Seismological Society of America*, **85**, 1275-1284.
- Nigam, N. C. and Jennings, P. C., 1969, Calculation of response spectra from strong-motion earthquake records, *Bulletin of the Seismological Society of America*, **59**, 909-922.
- Sharp, R. V., Rymer, M. J. and Lienkaemper, J. J., 1986, Surface displacement on the Imperial and Superstition Hill faults triggered by the Westmoreland, California earthquake of 26 April

- 1981, *Bulletin of the Seismological Society of America*, **76**, 949-965.
- Shome, Nilesh., Cornell, C. A., Bazzurro, P. and Carballo, J. E., 1998, Earthquakes, records and nonlinear response, *Earthquake Spectra*, **14**, 469-500
- Shome, Nilesh and Cornell, C. A., 1998, Normalization and scaling accelerograms for nonlinear structural analysis, in *Proceedings, 6th U. S. National Conference on Earthquake Engineering, Seattle Washington, May 31-June 4, 1998*.
- Stepp, J. C., Silva, W. J., McGuire, R. K. and Sewell, R. T., 1993, Determination of earthquake design loads for a high level nuclear waste repository facility, in *Proceedings, 4th DOE Natural Phen. Haz. Mitig. Conf., Vol 2, Atlanta, GA*, 651-657.
- Uang, C.-M. and Bertero, V. V., 1990, Evaluation of seismic energy in structures, *Earthquake Engineering and Structural Dynamics*, **19**, 77-90.
- Wald, D. J. and Heaton, T. H., 1994, Spatial and temporal distribution of slip for the 1992 Landers, California, earthquake, *Bulletin of the Seismological Society of America*, **84**, 668-691.
- Wald, D. J., Heaton, T. H. and Hudnut, K. W., 1996, The slip history of the 1994 Northridge, California, earthquake determined from strong-motion, teleseismic, GPS, and leveling data, *Bulletin of the Seismological Society of America*, **86**, no. 1B, 49-70.
- Wessel, P., and Smith, W. H. F., 1991, Free software helps map and display data, *EOS Trans. Amer. Geophys. U.*, **72**, 441, 445-446.

#### BIBLIOGRAPHY OF PUBLICATIONS RESULTING FROM THIS WORK

- Chapman, M. C., 1998, The potential use of an energy-based motion parameter for probabilistic seismic hazard analysis, Abst., *Seismological Research Letters*, 69, no. 1, 76
- Chapman, M. C., 1998, An energy-based motion parameter for probabilistic determination of scenario earthquakes, Abst., *Seismological Research Letters*, 69, no. 2, 173.
- Chapman, M. C., 1998, On the use of elastic input energy for seismic hazard analysis, manuscript submitted for publication to *Earthquake Spectra*, September, 1998.